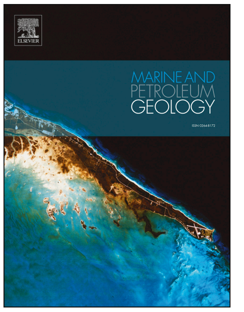

The Global Middle and Late Miocene and the Deep Earth: Model for Earlier Orogenies

Paul Edwin Potter, Peter Szatmari

PII: S0264-8172(15)30073-8

DOI: 10.1016/j.marpetgeo.2015.08.021

Reference: JMPG 2329

To appear in: *Marine and Petroleum Geology*

Received Date: 19 March 2015

Revised Date: 11 August 2015

Accepted Date: 15 August 2015

The Global Middle and Late Miocene and the Deep Earth: Model for Earlier Orogenies

Paul Edwin Potter

Geology, University of Cincinnati, OH 45221, USA

Peter Szatmari

Petrobras Research Center, Ilha do Fundão, Rio de Janeiro, RJ, 21949, Brazil[*]

Key Idea—The 50-some diverse events of the Middle and Late Miocene reported here are best explained by combining the deep earth cycle first proposed by Arthur Holmes in 1929 and 1944 with modern, deep seismic tomography.

Abstract: The 11 Ma Middle and Late Miocene interval forms only 2% of Phanerozoic time but includes two broadly contemporaneous global orogenies—one reaching across southern Eurasia and the other spanning the Circumpacific. These two global orogenies caused many global events, and because they are close to us in time, causality links between these orogenies and these far scattered events are much more apparent than in older orogenies. These teleconnections include establishment of the present world oceanic current system; the beginnings of oceanic cooling at 14 Ma; an increase in hemipelagic mud bordering the continents; changes in continental tilts and river systems; great biological changes; increased

[*] Corresponding author is Szatmari and his email is szatmari@petrobras.com.br

desertification; replacement of C_3 by C_4 grasses; a major shift in siliceous microfossils from the Atlantic to the Pacific at 15 Ma; and first development of the earliest hominids in East Africa starting at 10 Ma. In addition, spreading rates of oceanic ridges increased, volcanism increased, there was movement along many transform faults, and continental elevations increased. Short, bulleted statements set forth these near and far field events.

Immediate causes were increased rates of plate motions and/or changes of directions. Only a strong, short 11 Ma pulse of heat from the Earth's core provides the logical ultimate source of this energy. Only such a pulse of heat from the core has sufficient magnitude and acts globally. Thus the deep Earth cycle is a plausible, easy-to-understand, overarching explanation that should be increasingly considered by geologists and geophysicists studying the outer crust. A flow diagram links major earth surface features on the continents to the deep earth. Alternative explanations for these events are considered and seem totally inadequate.

Introduction

We propose that the major events in Miocene oceans, atmosphere, and continents are all related to plate tectonics, and that these events in turn, are linked to the deep earth cycle as an integrated system extending far back in time. Demonstration of Miocene connections to the deep earth will go far to help identify similar connections in earlier global orogenies.

There are two reasons why understanding the interrelationships among the many synchronous global events from the base of the Middle Miocene (Langhian) to the end of the Late Miocene (Tortonian-Messinian) from 16 to 5.3 Ma (Fig. 1), best demonstrate the links between the earth's surface features and its deep earth cycle. First, the Middle and Late Miocene are close to us in time, so their major tectonic processes and consequences are readily studied, making causality links easier to identify than those in earlier orogenies. Second, many, if not most, of the diverse global events of the Middle and Late Miocene are either directly or indirectly related to only two major tectonic events: the Alpine-Himalayan and Circum-Pacific Orogenies (Fig. 2). In broad terms, these two orogenies marked the final replacement of a lingering greenhouse world by an icehouse world. Advances in deep earth seismic tomography link both of these orogenies to the deep earth's major cycle, first proposed by Arthur Holmes in 1929 and 1944.

Global Setting

The Alpine-Himalayan and Circum-Pacific global orogenies both formed over subduction zones along oceanic margins, and both contain new and rejuvenated mountain belts, some of the latter as recent as 84 to 37 Ma (Gries, 1983; Getz, 2012), the widespread Laramide Orogeny (North America). The Alpine-Himalayan Orogeny extends from Gibraltar into Vietnam, some 13,000 km. This orogeny resulted from the African, Arabian, Indian and Australian Plates impacting southern Eurasia as Gondwana broke up and its fragments moved north over approximately 120 Ma to finally close the Tethys Ocean in the early Miocene. Today, only the Mediterranean, Black, Caspian, and Aral Seas, and some smaller lakes to the east remain. South America first rifted and opened from Africa between 135 and 120 Ma ago. This initial narrow gulf opened northward to finally connect with the central Atlantic, forming a proto-Atlantic Ocean at about 58 Ma (Scotese, 2000).

The Circum-Pacific orogenic belt, on the other hand, is 29,000 km long and also formed over subduction zones along the margins of the Pacific Ocean, but with a most significant difference: along the western and northern margin of the Pacific from New Zealand to Alaska, where oceanic crust is oldest and coldest (Sclater et al., 1985, Fig. 3), retreat of the subducting plates was accompanied by the formation of interarc and backarc basins. These basins have complex tectonism that included seafloor spreading and multiple subduction zones. From Gibraltar eastward along the border of southern Laurentian Asia, the impact of north-moving fragments of Gondwana—the African, Arabian, Indian, and Australian Plates—formed mountain chains such as the Atlas, Alps, Carpathians, Zagros, Himalayas, and those of Vietnam and Thailand. These two global Miocene orogenic belts are largely built on an earlier global orogeny of Late Cretaceous-Early Eocene age with modifications in and near the Oligocene-Neogene boundary (Levin, 1994). Although collisions started as early as the Permian, much of the present tectonic configuration of southern Asia traces its origin to the first docking of India that began at about 50.5 Ma (Green et al., 2008). This impact finally produced the great change in sedimentary strike around the east end of the Himalayas, with its many strike-slip faults, and the dominantly north-south grain across Vietnam and Thailand that controls much of its principal drainage. Similarly, the northward drift of the Australian and Indian Plates produced the major tectonic features of the Indonesian archipelago. All of these broadly contemporaneous events are associated with major subduction zones and clearly require a deep earth cause. Renewed heating and upwelling along the margins of the two large, low shear velocity provinces, the African and Pacific Superswells (Fig. 2), are the ultimate drivers of these global events. See Potter and Szatmari (2009, 2012) for earlier, initial discussion of these events.

Middle and Late Miocene Events

Many of these teleconnections are proximal to major near field tectonic events, such as an orogenic front or transform fault, whereas others are far field events, such as the closing or opening of a key but distant isthmus, a far-ranging change in continental tilt, the growth of a large rain shadow as a major mountain range rose or the development of a monsoon as a jet stream was deflected. Most, but not all, of these events started in either the Middle or Late Miocene, but also included are a few long term (many millions of years) events associated with processes dating from the breakup of Pangea (about 200 Ma) or from the Oligocene and continued into and through the 11 Ma of the

Middle and Late Miocene. Many of these display an increase of intensity in the Middle or Late Miocene. The events below can be thought of as a check list – what to look for or consider when studying, and especially when modeling, earlier global orogenies. An early demonstration of these global teleconnections with respect to intercontinental uplift and climate was provided by Ruddiman et al. (1989); see Chapin (2009) for a comprehensive example in the southwestern United States, who integrated both on and off shore events.

Tectonic

- The Middle Miocene saw increased spreading rates (Kominz, 1984, Fig. 3A) as well as one of the fastest spreading rates of 180 to 210 mm/yr observed on the ocean floor in the Cocos Plate (Wilson, 1996). Logically, faster spreading rates of mid-ocean ridges imply increased tectonic activity at and along convergent and transform margins and probable enhanced activity in continental interiors as well.
- Heightened and new activity of the Circum-Pacific and Atlas-Alpine-Zagros-Himalayan global orogenic belts, totaling some 42,000 km, formed high mountains and plateaus and globally shed immense quantities of mud and sand (Dickinson et al., 1986 and our Fig.2).

- The Tethyan Ocean (Fig. 3) was closed by fragments of Gondwana, first by India during the Eocene at 50.5 Ma (Green et al., 2008), intermittently isolated the Mediterranean from the Tethys in much of Miocene (Ziegler, 1988; Rogol, 1999;) and temporarily closed Gibraltar during the latest Miocene at 5.3Ma (Maldonado and Nelson, 1999, p.229). This long interval of closing is a tectonic event comparable to the two global orogenies, because it concentrated the continents in the northern hemisphere, formed the gigantic accretionary margin of southern Eurasia, and disrupted the long-lived global equatorial current (Perrin, 2002, Fig. 5 and Smith and Pickering, 2003).

- The global orogeny formed many new sedimentary basins while older ones were uplifted (inverted) and eroded.

- Wide epeirogenic uplift of continental interiors and many passive margins (but not everywhere) helped cool the atmosphere and accelerate erosion. Examples include the uplift of British Columbia at 10 Ma (Farley et al., 2001), the Rocky Mountains (Christiansen and Yeats, 1992), the 10 Ma uplift in the central Andes (Garzione et al., 2008), the replacement of tropical forest in northeast Africa by semiarid landscape in response to uplift at 10 Ma (Sakai et al., 2010, Fig. 9), the uplift of the north Tibetan Plateau since 15 Ma (Li et al., 2011), the Central Range Orogeny of New Guinea at 12 Ma (van Ufford and

Cloos, 2005), and as summarized by Dooley et al. (2013), the Middle and Late Miocene epeirogenic uplift of much of the interior and coastal regions of the southern United States.

- The climax of long-term, northward drift of Gondwana's fragmented continents led to seven stepwise major openings and closings of ocean gateways (Fig. 3), and finally ended the earlier warm, global, homogenizing equatorial current (Smith and Pickering, 2003). This fundamentally rearranged the earth's atmospheric heat balance.
- The Japanese archipelago assumed its present form largely in the Middle Miocene (Takahashi and Oda, 1997, Fig. 3).
- Central America initially connected to South America in the Middle Miocene judging by U-Pb ages of zircons (Montes et al., 2015).
- On the east side of the North Pacific in the "mid Miocene," there was a transition across the Cordilleran region of the western United States from Laramide tectonics to strike slip and extensional tectonics (Christiansen and Yeates, 1992, p. 261).
- Many major, large transform faults on or near the continents were reactivated or initiated, and by inference, so were those at sea. Two onshore examples

are the Dead Sea Transform, whose main movement began in the Middle Miocene (Kesten et al., 2008), and the Great Alpine Fault between the Australia and Pacific Plates of New Zealand began in the Early Miocene (King, 2000) both of which continue to this day.

- Block faulting began in the Basin and Range Province of the western United States between 17 and 15 Ma, followed by later spreading (Fosdick and Colgan, 2008).

Volcanic

- Widespread volcanism occurred not only along midocean ridges (Saemundsson, 1986) and ocean-continent convergent margins, but also on the continents and in some intraplate regions.
- The Colombia basalts started just before the Middle Miocene (17 Ma) fed by the rupture of the descending Farallon slab (Liu and Stegman, 2012).
- Two examples of Miocene intraplate volcanism are the Colombia River basalts-greater Yellowstone region and the greater Mediterranean regions (Fig. 4). Notice the sharp increase of Miocene activity in the greater Mediteranean area in the Middle and Late Miocene.
- Early seismic image (Fig.5) of the shallow upper mantle plume beneath the modern Yellowstone volcanic field is probably typical of other hotspots, past and present.

Global Climate and Oceans

- Conjunction of opening and closing of seven tectonic gateways, clustering of continents at northern high latitudes, and higher continental interior elevations initiated cooling of the global ocean and atmosphere between 15 and 14 Ma greatly altered the world's temperature regime (Zachos et al., 2001; Miller et al., 2005), a most significant inflection point in Cenozoic earth history (Fig. 6). A good specific example is provided by the entry of cold water into the North Atlantic at the beginning of the Middle Miocene (Wright and Miller (1996, p. 161).

- Principal features (locations, intensities, and temperatures) of much of present global oceanic circulation developed concurrently with the expansion of the Antarctic ice sheet between 15 and 14 Ma in the early Middle Miocene (Keller and Barron, 1983).

- Near the base of Middle Miocene the ocean became more oxic in response to its new more energetic circulation (Norris et al. 2013, Fig, 2).

- The withdrawal of the Tethyan Ocean was almost completely established by the late Middle Miocene (Keller and Barron, 1983).

- Major eustatic falls in global sea level occurred in the Middle and Late Miocene with Antarctic ice advances an important cause Bartek et al. (1991). See widely separated examples both in clastics (Greenlee and More, 1988) and carbonates (Betzler et al., 2000 and Tcherepanov et al., 2008). Sea level fall at the base of the Tortonian is notably widespread and is inferred to result from a large advance of East Antarctic ice (Flower and Kennett, 1994.

- Deep-water unconformities, disconformities, and hiatuses developed when shorelines retreated below the shelf edge bringing stronger currents to deeper waters forming subsea turbidite fans and disconformities; in the Middle Miocene there was some extensive carbonate dissolution of calcareous bottoms—the “carbonate crash” of the Caribbean (Roth et al., 2000 and Keller and Barron, 1983).

- Rise of the Tibetan Plateau shifted the Asian jet stream to form the monsoon. Aided by the withdrawal of the Paratethyan Ocean from central Asia and new uplifts with rain shadows (QuI, 2014). Chinese loess started at 22 Ma (Guo et al., 2002). Most of southwestern Asia and the Sahara became drier in the Tortonian as the Tethys closed (Zhang et al., 2014). In northeast Africa epeirogenic uplift induced dryness (Wichura et al., 2010).

- The Middle Miocene Climatic Optimum at 17.0 T0 14.7 Ma is widely reported across the world (Hilgren et al., 2012, Fig. 29.13).
- Mountain glaciation spread as the Miocene cooled and supplied thick, poorly sorted clastics to high-latitude marginal marine basins with deposits such as the Yakataga Formation (Armentrout, 1983; Eyles et al., 1991), and to large cratonic rivers with glaciated watersheds.

Clastic Deposition

- Sedimentation rates in the ocean greatly increased during the Middle and Late Miocene (Davies et al., 1977), along with increasing amounts of Al_2O in deep-sea muds (Donnelly, 1982) as Middle and Late Miocene deltas thickened and expanded; e.g., the Orinoco (Di Croce, 1995, Fig.3.3b) and the Gulf Coast (Galloway, 2008). In the Gulf of Mexico clastics increased in the late Early Miocene and again in the Late Miocene (Galloway et al., 2015, Fig. 20).
- Shorelines prograded markedly along passive margins with many clinothems and new and enlarged continental embankments (Fig.7). Near the continents there was enhanced hemipelagic mud deposition (Donnelly, 1982).
- The Middle and Late Miocene was a time of great tectonically induced change in river systems, and new

and enlarged older deltas, and subsea fans (Fig. 8), especially on passive margins (Potter and Hamblin, 2006).

- Large falls in global sea level in the Miocene shifted sand deposition from shelf or platform to lower slope and deep water, as happened at the base of the Tortonian of the Gulf of Mexico, West Africa, and elsewhere. This progradation beyond the shelf edge onto the lower continental slope caused mass gravity sliding (enhanced over steepening and overpressure) at lowstands (Fig. 9). Large deep sea fans such as those of the Amazons developed at the same time.
- Principal sedimentary fill of the western Pacific back arc basins occurred in the Miocene after volcanic dominance that started in the Oligocene.
- Stepwise flooding of mud to global oceans in the Miocene is well defined at 16 Ma by a sharp rise in $\delta^7Li^0/_{00}$ (Misra and Froelich, 2012, Fig. 4.b), based on many hundreds of samples from benthonic foraminifera (Fig. 10).
- A new disjointed and invigorated ocean current system (Fig.3) introduced cold polar waters to lower latitudes and caused many deep-sea hiatuses and unconformities and increased upwelling of cold nutrient rich water. These new areas of Miocene upwelling in the Pacific

formed the organic rich shales off Sakhalin Island and the Middle Miocene Monterey Formation of California.

Landscape

- Globally, Middle and Late Miocene tectonic activity left two major global landscapes: a near-field tectonically altered Miocene alpine landscape with a far-field landscape (vast aprons, llanos, and steppes in the Northern Hemisphere), plus a relic, little-altered Gondwana landscape quite different from much of today's glaciated Northern Hemisphere (Squires, 1988).
- Middle and Late Miocene tectonism shifted continental tilts and divides in response to accelerated plate motions and new uplifts and continental tilts.
- Some preexisting rivers were destroyed and many new ones formed, along with their associated deltas and subsea fans. A few examples of new Middle and Late Miocene rivers include the Amazon, Amur, Columbia, Danube (and those flowing north and west away from and in Alps and Carpathians), Orinoco, and Magdalena plus the Nile canyon. (Potter and Hamblin, 2006, Fig.16).
- Sharpened climate contrasts developed on continents: large rain shadows with deserts and loess and growth of mountain glaciation, all were concurrent with global oceanic and atmospheric changes and glaciers expanded in Antarctica.

Groundwater

- Back tilting of adjacent platforms and cratons can shift or reverse the direction of subcontinental groundwater during an orogeny in adjacent foreland and cratonic basins (Garven, 1992; Nunn and Lin, 2002). Such reversals may lead to distal, far-field, mineralized fracture systems as hot acid fluids expelled from marginal highlands cool in carbonate platforms such as in the Trenton carbonates (Acadian Orogeny) of the northeastern United States and Canada (Smith and Davies, 2006; Davies and Smith, 2006).

Biology

- **R**apidly changing paleoclimates, paleo-oceans, and paleogeography greatly increased environmental stresses on land and sea, caused not only accelerated evolution (horses, cats, hominids, etc.), but also major shifts in fauna and flora and greater diversity. See Kauffman (1976) and the summary by Hoorn et al. (2013).

- C_4 grasslands rapidly began to replace C_3 grasslands 8 to 3 Ma ago, one of the most rapid bionomic changes in the geologic record (Edwards et al., 2010). This altered erosion rates and sediment yields (shallower root systems).

- The biotic consequences of the opening and closing of gateways can be far-reaching, both in the oceans and on land; as the Isthmus of Panama closed, siliceous microfossils shifted (the silica shift) from the Atlantic to the Pacific Ocean (Keller and Barron, 1983, Fig. 13), and the Central American tiger displaced the terror bird (Kespka, 2014, p. 37) as the dominant predator of South America.
- Uplift in East Africa at 10 Ma set the stage for early hominid evolution (Fig. 11).
- Dissolved oxygen increased deep-sea benthonic foraminifera test size at 16 Ma (Kaiho, 1998, Fig. 3).
- Reef sites started to decline at about 12 Ma during the Serravallian (Perrin and Kiessling, 2010).
- Starting at 10 Ma, the flood of Andean mud and silt into the tropical western Amazonia region changed nutrient-poor tropical soils into nutrient-rich Andean soils, greatly enriching their microbiology and fauna and flora (Hoorn et al., 2010).
- The present dominance of red algal reefs started in the Burdigalian and expanded in the Middle Miocene (Halfar and Mutti, 2005).
- At 74° N on Banks Island in the Arctic Archepelego a pine forest growing in lower middle Miocene beds started to decline (Williams et al., 2008)

Petroleum

- New or enlarged deltas and deep-sea fans provided reservoir beds and reservoirs so that today the Middle and Late Miocene, with a duration of only 11 Ma (only 2 percent of Phanerozoic time), hosts about 17 percent of the world's petroleum. Equally important, prolific Middle and Late Miocene sedimentation buried underlying Cretaceous organic-rich shales to form petroleum source rocks.
- In the Middle Miocene, lowering of sea level shifted deposition from the platform to the continental slope and beyond to form many of today's deep-water reservoirs in the Gulf Coast (Galloway, 2008) and elsewhere. Rapid muddy sedimentation on these unstable slopes induced sliding of large slabs of slope sediment on the Gulf Coast and Niger delta with extensional faulting at their heads and frontal fold-and-thrust belts.
- Synsedimentary diapirism and trap formation occurred during rapid burial above weak, thick mud or salt on continental shelves and slopes (Miocene of northern Gulf of Mexico, as well as in the Niger delta, Trinidad, Azerbaijan, and Indonesia).
- Diatom reservoir rocks of the Miocene Monterey Formation and those of Sakhalin Island accumulated in

the Middle Miocene as cold, nutrient-rich water upwelled against continents.

- Far-field, mineralized fracture systems and wrench faults related to major orogenies may harbor secondary dolomitic reservoirs (Smith and Davies, 2006).
- Because of a flood of clastics, there are only 197 carbonate petroleum reservoirs in Early and Middle Miocene deposits whereas there are 348 in Late Miocene deposits (Markello et al., 2008, Fig.5) – suspended mud inhibits filter feeders.

Proximate Causes

Collectively, the events and teleconnections cited in the above observations reveal the amazing number and diversity of the events related to Late and Middle Miocene atmospheres, oceans, biology, and surface geology, all of which transformed a lingering greenhouse world into an icehouse world. Especially notable is their short time span, only 11 Ma, in comparison to the Laramide Orogeny of 84 to 37 Ma years in the Americas.

The vast majority of these events are directly or indirectly linked to plate motions—the placement of continents with respect to each other and the poles, whether continents have convergent, transform, or passive margins or develop major rift systems. All of these rearrange oceanic circulation systems by opening and closing key gateways, shutting off or opening cold or warm water and possibly altering their nutrients and oxygen content and velocity. It is plate motion that directly forms major mountain belts, energizes transform faults, and both forms new sedimentary basins and destroys others. Continental tilts are also directly related to plate motions and are responsible for many other significant features, such as the orientation and locations of large, subcontinental river systems and their associated deltas and subsea fans, flooding much of the world ocean with mud and helping build thick wedges of continental embankments on the margins of continents. The topographic deflection of jet streams by rising mountains (Southeast Asia, Andes) and far-reaching rain shadows of high mountains or plateaus provide other examples. Global orogenies also favor more mountain glaciation and seem important for middle latitude ice sheets too. Volcanism is also a major feature of ocean-continent convergence as it correlates with ridge spreading rates, and also occurs in intraplate settings (Fig. 4); more plume and hotspot activity is responsible for much of this. These rapid and extensive changes of paleogeography during global orogenies caused extensive evolutionary changes and many shifts of flora and fauna. The short time of 11 Ma for all these events *points to a single cause.* The global scope of these events in this short time reinforces this inference. We argue that the great global reach and broad, global 11 Ma contemporaneity of the above Miocene events are *best explained by a sharp, short strong pulse of heat from the earth's core.* That this pulse of heat was global in scope was first suggested by Mjelde and Faleide (2009), who proposed co-pulsation for the magma fluxes of the Hawaii-Emperor Ridge in the Pacific and the Iceland hotspot in the

Atlantic; similar antipodal co-pulsation can be noted also between the Ontong-Java LIP in the Pacific and the Parana-Etendeka LIP that preceded the South Atlantic.

Machinery of the Deep Earth Cycle

The machinery of the deep earth, first proposed by Holmes (1944), has since become increasingly sophisticated, mainly by studies of seismic tomography. This shows that the Earth's surface history is controlled by the dynamics of the mantle. Subducted plates formed by the amalgamation of supercontinents periodically collapse to form the high-velocity D" layer, a slab graveyard at the core mantle boundary (Maruyama et al., 2007; Fig. 12). Heat from the core in time partial melts this layer, causing andesitic solids to rise, forming large low shear velocity provinces or superplumes. Large igneous provinces have been generated by plumes rising from the steep margins of these LLSVPs (Fig. 13; Courtillot et al., 2003; Anderson, 2007; Torsvik et al., 2006; Li and Zhong, 2009; Foulger, 2010). The position of these two antipodal Large Low Shear Velocity Provinces (LLSVPs), one below Africa and the other below the central Pacific, correlate with dynamic topographic highs or superswells (Figs. 2, 12, and 13) that may have remained constant for hundreds of millions of years while plates migrated above them (Torsvik et al., 2006; Burke et al., 2008). Alternatively, proxy modeling indicates that the LLSVPs and thermochemical "superplumes" may have been easily swept away by cold subducting slabs throughout the

Phanerozoic, moving over the free-slip surface of the liquid outer core (McNamara & Zhong, 2005, Zhang et al., 2010).

Other examples of this inferred linkage between earth surface features and those of the deep earth include: (1) the reversal of the Amazon River (continental drifting over a sinking slab; Shepard et al., 2010); (2) origin of the Columbia River basalt (rupture of the Farallon slab; Liu and Stegman, 2012), (3) flooding history of the Australian craton in the last 70 Ma (sinking slab and proximity to Melanesian subduction; Heine et al., 2010); (4) coupled uplift of the Colorado Plateau and the less dense/hotter mantle underlying high areas of the Rocky Mountains (Karlstrom et al., 2012); (5) development of a regional drainage system in Paleocene-Eocene mudstone north of Scotland (in response to passage of the Icelandic plume; Hartley et al., 2011); and (6) modeled reconstruction of the last 30 Ma years of mantle topography of Africa's basins and rifts (Moucha and Forte, 2011). Another example is provided by basin evolution above a shallow rising mantle plume (Fig. 13). See Hager et al. (1985), Braun (2010), Allen (2011), Jones et al. (2012), Cloetingh and Willet (2013) and Kerr (2013) for a discussion of the effects of the mantle on dynamic topography.

What does the deep earth literature tell about a possible cause of the abrupt increase in global tectonic activity at the beginning of the Middle Miocene? As far as we know, this question has not been asked or discussed in detail in the literature. The recent recognition that the core has thermochemical cycles just as does the mantle (Maruyama et al., 2007; Aubert et al., 2008) is a possible pathway to an explanation for this short, abrupt, global pulse of heat. Could it be that the simultaneous heat pulse we infer for the two superplumes resulted from a brief spatial superposition of both mantle and core cycles, one heat maxima briefly positioned under the other?

Our hypothesis of a pulse of heat from the Earth's core as the cause for the Middle and Late Miocene events finds support in the recent work by Pozzo et al. (2012, 2014) who used density functional theory to compute thermal and electrical conductivities in liquid iron mixtures at core conditions from first principles. They found the conductivities of both cores to be two to three times higher than those currently used, concluding that the adiabatic heat flux is 15 to 16 terawatts at the core mantle boundary (CMB). Building on these results, Morgan and Vanucchi (2014) showed that an approximate 500-1000 g/m^3 seismically-inferred increase in density between the liquid outer core and solid inner core allows us to directly infer the core-freezing Clapeyron Slope (temperature-pressure ratio during phase change) for the outer core's actual composition which contains ~approximately 8±2% lighter elements (S,Si,O,Al, H,...) mixed into a Fe-Ni alloy. Basing their Clapeyron Slope on the 600 kg/m^3 jump between outer and inner core (Preliminary Reference Earth Model PREM; Dziewonski & Anderson, 1981), Morgan and Vanucchi (2014) concluded that there has been approximately 774K of core cooling during the freezing and growth of the inner core, releasing approximately 24 TW of power during the past 3 Ga; such high heat flow across the core-mantle boundary (CMB) means that the present-day mantle is strongly 'bottom-heated' so that *diapiric mantle plumes should dominate deep mantle upwelling.* Like diapiric mantle plumes, core convection is also pulsating. This fully supports our hypothesis that a "pulse of heat" from the core was the power source for global orogenic events such as those of the Middle and Upper Miocene.

Flow Diagram for the Continents

The flow diagram of Figure 15 outlines the principal causal connections between the deep earth and its surface geology on the continents—crustal tectonics connected to the deep Earth cycle. We suggest that Figure 15 applies to all of Phanerozoic history and well into the Neoproterozoic. Uncluttered by many secondary feedback loops, this diagram identifies only the main pathways of causality on the continents and thus provides an easy-to-understand way to see how heat from the earth's core drives its surface geology. Faster plate motions and more plume and hotspot activity were the immediate drivers of the burst of activity in the Middle and Late Miocene that laid the foundations of our modern world. Most of these events and their associated processes occurred within the 11-Ma interval of the Middle and Late Miocene and thus were either partially or totally overlapping—certainly itself strong evidence for a deep earth cause. Figure 15 also lists the principal volcanic areas on the continents since the Triassic-Jurassic boundary, which have long been linked to underlying plumes (Kerrick, 2001).

Seven immediate major controls on global paleogeography that are most directly related to plate tectonics and the deep earth include (1) the configuration (clustering and shape) and position of the continents, (alter the earth's heat balance and polar ice sheets reduce global sea level); (2) global and subcontinental orogenies alter continental elevations, tilts, watersheds, and jet streams; (3) uplifts of continental interiors and passive margins change drainage; (4) tectonic openings and closings of oceanic gateways change global oceanic circulation and thus world climate. And what can be said of local relative sea level, as the immediate control to shifting shorelines and cycle stratigraphy? Here tectonic control is less direct, because shoreline shifts depend on the interplay of basin subsidence (accommodation), supply, and changes of eustatic sea level. Even here, however, sub-lithospheric mantle temperatures can strongly modify the local sea level curve, as along the New Jersey coastline. Plate tectonics also has significant influence—it can directly alter eustatic sea level through changes of mid-ocean ridge volumes, or less directly, by causing global cooling, leading to expanded polar ice sheets. In sum, plate tectonic controls on eustatic sea level are simply more modulated and thus less direct than either global orogenies, polar clustering of the continents, or widespread epeirogenic, continental uplifts.

Possible Alternative Explanations

Let's test the above summary and explanation of Middle and Late Miocene events by exploring two alternatives.

One possibility is simply more rainfall in the Middle and Late Miocene – were these 11 Ma years wetter or dryer than earlier in the Tertiary? Evidence about rainfall comes from stratigraphy and regional geology. The first loess in Northwest China is dated at 22 Ma (Guo et al., 2002), in response to a rising Tibetan Plateau followed by the withdrawal of the Peri-Tethyan Ocean across Kazakhstan and neighboring countries. Although some aridity is reported earlier around Lake Chad (Schuster et al., 2006), desertification accelerated in the late Miocene in the Sahara, across southwest Asia. In North America, desertification started in the late Middle Miocene, and some 5 Ma later in Europe (Eronen et al., 2012). By the Late Miocene, desertification was advanced in coastal Peru and Chile and rain shadows existed in front of the Andes. During the Tertiary Australia drifted northward and in the Miocene had a climate broadly similar to that of today. Thus, with the possible exception of the brief Middle Miocene warm period, stratigraphic and landscape evidence points to a drier rather than a wetter Middle and Late Miocene climate—making a worldwide increase in rainfall a most unlikely cause of more Middle and Late Miocene clastics.

In a pioneer paper in 1990, Molnar and England suggested another alternative: late Cenozoic cooling as an alternative cause of worldwide uplift and increased sediment supply. They reasoned as follows. Today's high mountains may result from lower temperatures leading to expanded mountain glaciers, stronger and wider mid-latitude storm tracks (altered jet streams), more variable humidity, and different vegetation, all causing more erosion. This would increase isostatic uplift and in turn lead to more erosion and sedimentation. A voluminous and conflicting literature has since followed as summarized by Whipple (2009) and Owen (2013). Most of these studies are of single mountain ranges. Herman et al. (2013), however, compiled 17,833 fission tracks of apatite and zircon from around the globe and clearly established an increase in sedimentation rates since 8 Ma, and especially since the Pleistocene with its more widespread mountain glaciation. Thus, mountain glaciation is and was a factor in the past. But think of all the Middle and Late Miocene tectonic events reviewed above — reorganization of the tectonics of the Middle Miocene in the western United States, the consolidation of the Japanese archipelago between 16 and 14 Ma, the accelerated spreading of mid-ocean ridges in the Middle Miocene, the lava-induced subsidence of the Greenland-Iceland-Scotland gap (released cold arctic water into the world ocean), the long-term closing of the Isthmus of Panama, the marked increase in Middle Miocene volcanism in western Europe and the Mediterranean area, as well as the initial extrusion of Columbia Plateau basalts at 17 Ma. All of these are major features of the modern world, as are the uplift and faster movements of its mountainous, convergent plates. From another point of view, think of the Late Miocene uplift of the North Range of New Guinea, the Late Miocene emergence of Taiwan, or the uplift of

East Africa starting at 10 Ma—none of which are glaciated. It seems most improbable that isostatic uplift, driven by deep glacial erosion, could have had a comparable role. Can the climate-glacier argument be more than a small secondary enhancement?

One last question remains—how long did the inferred pulse of Middle and Late Miocene heat flow last? Do we still have it or has it ceased? We did not explore this question, but we did find—totally by accident—some research on it in the diatomaceous, offshore Neogene beds of the northeast Atlantic Ocean near the Faeroe and Shetland Islands (Davies and Cartwright, 2002). Utilizing both the temperature-dependent transition of amorphous (opal A) to crystalline (opal CT) and seismic data, they inferred higher burial temperatures (opal CT) from the base of the Middle Miocene to the top of the Late Miocene, which is separated from the early Pliocene by an unconformity. The early Pliocene beds only have opal A—in other words; during the time interval of the unconformity, heating ceased. More attention to Neogene heat flow and its relations to the Earth's surface seems most worthwhile.

Summing up, none of the above alternatives come as close to explaining the many diverse Middle and Late Miocene events and their flood of clastics and teleconnections than globally reactivated plates. The most logical source for this needed energy is *a short 11 M pulse of heat from the earth's core.*

Conclusions

- The two closely synchronous global Middle and Late Miocene orogenies caused many global near- and far-field teleconnections on the continents, in the oceans, and in the atmosphere in only 11 Ma. Virtually all of these global events are best explained, either directly or indirectly, by plate tectonics.
- The only source for increased global plate activity is an intense pulse of energy—a sharp, strong burst of heat from the earth's core—transferred upward by conduction through the D" boundary layer into the mantle and then by plumes into the lithosphere and its plates.
- The global teleconnections of the Miocene identified in our research make them the ideal standard for what to look for, when studying earlier basins or earlier major orogenies far back into Neoproterozoic time.
- Broader awareness of the teleconnections reported here is the first step toward identifying many, many more in the Earth machine.

Although most practical significance is yet to come, it seems clear that in the near future many more explanations of surface geology will increasingly incorporate insights from deep earth seismic tomography. When this happens, practicality should be close at hand.

Acknowledgments

We are most pleased to acknowledge the many, who have helped us over the years. Foremost are both the Geology Department of the University of Cincinnati and PETROBRAS/CENPES, Rio de Janeiro, RJ, Brazil, for their sustained support, without which we could not have prepared this manuscript. Critical readers include William van Wie, consultant, Houston, Texas; and Kevin Bohacs, Exxon Mobil Upstream, Houston, Texas plus Lewis Owen and Barry Maynard of the University of Cincinnati. Helpful outside reviewers were Dimitry A. Ruban, Southern Federal University, Rostov-na-Donu, Russia and Patrick G. Eriksson, Geology, University of Pretoria, South Africa. Essential support was provided by our university librarians, Holly Prochaska and June Taylor—countless interlibrary loans—and the skills and patience of our designer, Timothy Phillips. Many, many thanks to all/muito, muito obrigado a todos!

References Cited

ALLEN, P.A. (2011) Surface impact of mantle processes. *Nature Geoscience*, **4**, 498–499.

ANDERSON, D.L. (2007) *New theory of the earth.* Cambridge University Press, Cambridge, UK.

ARMENTROUT, J.M. (1983) Glacial lithofacies of the Neogene Yakataga Formation, Robinson Mountains of southern Alaska Coast Range. In: *Glacial-Marine Sedimentation,* (Ed. by B.F. Molina). Plenum Press, New York, 421–449.

AUBERT, J., AMIT, H., HULOT, G., & OLSON, P. (2008). Thermochemical flows couple the Earth's inner core growth to mantle heterogeneity. *Nature*, **454**, 7 Aug. doi:10.1038/07109.

BARTEK, L.R., VAIL, P.R., ANDERSON, J.B., EMMET, P.A. & WU, S. (1991) Effect of Cenozoic ice sheet fluctuations in Antarctica on the stratigraphic signature of the Neogene. *J. Geophys. Res.,* **96**(B4), 6753-6778.

BETZLER, C., KROON, D. & REIJMER, J.J.G. (2000) Synchroneity of major late Neogene sea-level fluctuations and paleoceanographically controlled changes as recorded by two carbonate platforms. *Paleoceanography*, **15**, 722-730.

BRAUN, J. (2010) The many surface expressions of mantle dynamics. *Nature Geoscience*, **3**, 825–833.

Bull, A. L., McNamara, A. K., & Ritsema, J. (2009). Synthetic tomography of plume clusters and thermochemical piles. *Earth and Planetary Science Letters*, **278**(3), 152-162.

Burke, K., Steinberger, B., Ttorsvik & T.H., Smethurst, M.A, (2008). Plume generation zones at the margins of large low shear velocity provinces on the core-mantle boundary. *Earth and Planetary Science Letters*, **265,(**1-2),49-60.

Cartwright, J. (1995). Seismic-Stratigraphical Analysis of Large-Scale Ridge–Trough Sedimentary Structures in the Late Miocene to Early Pliocene of the Central North Sea. *Sedimentary Facies Analysis: a tribute to the research and teaching of Harold G. Reading*, 283-303.

CHAPIN, C.E. (2009) Interplay of oceanographic and paleoclimatic events with tectonism during the middle to late Miocene sedimentation across the southwestern USA. *Geosphere*, **4**, 976-991.

CHRISTIANSEN, R.L. & YEATS, R.S. (1992) Post-Laramide geology of the U.S. Cordilleran region. In: *The Cordilleran orogen: Conterminous U.S.*, (Ed. by B.C. Burchfiel, P.W. Lipmann & M.L. Zoebeck). *Geological Society of America, The Geology of North America*, G-3, 261–406.

CLOETINGH, S. & WILLET, S.D. (2013) Linking deep earth and surface geology. *EOS, Trans. Am. Geophys. Union,* **94**, 53–54.

COURTILLOT, V., DAVAILLE, A., BESSE, J. & STOCK, J. (2003) Three distinct types of hotspots in the earth's mantle. *Earth and Planetary Science Letters,* **205**, 295–308.

DAVIES, T.A., HAY, W.W., SOUTHAM, J.R. & WORSLEY, T.R. (1977) Estimates of world sedimentation rates. *Science,* **197**, 53–56.

DAVIES, R.J. & CARTWRIGHT, J. (2002) A fossilized opal-A to opal-CT transformation on the northeast Atlantic margin: support for a significantly elevated paleo-geochemical gradient during the Neogene? Basin Research **14**, 467-486.

Davies, G. R., & Smith Jr, L. B. (2006). Structurally controlled hydrothermal dolomite reservoir facies: An overview. *AAPG Bulletin* **90**(11), 1641-1690.

DICKINSON, W.R., SWIFT, P.N. & CONEY, P.J. (1986) Tectonic strip maps of the Alpine-Himalayan and circum-Pacific orogenic belts: Great circle projections. *Geol. Soc. Am. Map and Chart Series,* **MC-58**, 1:20,000,000.

DI CROCE, J. (1995) Eastern Venezuela Basin: Sequence stratigraphy and structural evolution. Rice University, Houston, Texas, doctoral dissertation, 225.

DONNELLY, T.M. (1982) Worldwide continental denudation and climatic deterioration during the late Tertiary: Evidence from deep-sea sediments. *Geology,* **10**, 451–454.

DOOLEY, T.P., JACKSON, M.P.A. & HUDEC, M.R. (2013) Coeval extension and shortening above and below salt canopies on an uplifted, continental margin: Application to the northern Gulf of Mexico. *Am. Assoc. Petroleum Geologists Bull.*, **917**, 1737–1764.

EDWARDS, E.J., OSBORNE, C.P., CAROLINE, A.E., STRÖMBERG, A.E. & SMITH, S.A. (2010) The origin of C_4 grasslands: Integrating evolutionary and ecosystem science. *Science,* **328**, 587–591.

ERONEN, J.T., FORTELIUS, M., MICHEELS, A., PORTMANN, F.T., PUOLMÄKI, K. & JANIS, C.M. (2012) Neogene aridification of the northern hemisphere. *Geology*, **40**, 823–825.

EYLES, C.H., EYLES, N. & LAGOE, M.B. (1991) The Yakataga Formation; a late Miocene to Pleistocene record of temperate glacial marine sedimentation in the Gulf of Alaska. In: *Glacial Marine Sedimentation, Paleoclimatic Significance,* (Ed. by J.B. Anderson & G.M. Ashley). *Geol. Society Am. Spec. Paper,* **261**, 159–180.

FARLEY, K.A., RUSMORE, M.E. & BOGUE, S.W. (2001) Post 10 Ma uplift and exhumation of northern Coastal Mountains, British Columbia. *Geology,* **29**, 99–102.

FONTANA, R.L. (1990) Investigações geofísicas preliminares sobre o cone do Rio Grande, Bacia de Pelotas-Brasil. *Acta Geologica Leopoldensia,* **13**, 161–170.

FOSDICK, J.C. & COLGAN, J.P. (2008) Miocene extension in the East Range, Nevada: A two-stage history of normal faulting in the northern Basin and Range. *Geol. Soc. Am. Bull.,* **120**, 1198–1213.

FOULGER, G.R. (2010) Plates versus plumes, a geological controversy. Wiley-Blackwell, Oxford, UK., 328p.

Galloway, W. E. (2008). Depositional evolution of the Gulf of Mexico sedimentary basin. *Sedimentary basins of the world*, **5**, 505-549.

Galloway, W. E., Whiteaker, T.L. & Ganey-Curry, P. (2015) History of Cenozoic North American drainage basin evolution, sediment yield, and accumulation in the Gulf of Mexico basin. *Geosphere* **7**, 938-973.

GARVEN, G. (1992) Continental-scale ground water flow and geologic processes. *Ann. Rev. Earth & Plan. Sci.,* **23**, 89–117.

GARZIONE, C.N., HOKE, G.D., LIBARKIN, J.C., WITHERS, S., MACFADDEN, B., EILER, J., GHOSH, P. & MUICH, A. (2008) Rise of the Andes. *Science,* **320**, 1304–1307.

GETZ, S.L. (2012) Impact of the Laramide Orogeny upon the petroleum geology of sedimentary basins north of the earth's equator. *Bull. Houston Geol. Soc.,* **54**, 31, 35, 37.

Green, O. R., Searle, M. P., Corfield, R. I., & Corfield, R. M. (2008). Cretaceous-Tertiary carbonate platform evolution and the age of the India-Asia collision along the Ladakh

Himalaya (Northwest India). *The Journal of Geology*, **116**(4), 331-353.

GREENLEE, S.M. & MOORE T.C. (1988) Recognition and interpretation of depositional sequences and calculation of sea-level changes from stratigraphic data – offshore New Jersey and Alabama. In: WILGUS, C.K., HASTINGS, B.S., ROSS, C.A., POSAMENTIER, H., VAN WAGNER, J., & KENDALL C.G. ST. C., EDS. SEPM SPECIAL PAPER NO. **42**, 329-353.

GRIES, R. (1983) North-south compression of Rocky Mountain foreland structures. In: *Rocky Mountain Foreland Basins and Uplifts,* (Ed. by J.D. Lowell & R. Gries). *Rocky Mountain Assoc. Geol.*, 9–32.

GUO, Z.T., RUDDIMAN, W.F., HAO, G.Z., WU, H.S., QIAO, Y.S., ZHU, R.X., … & LIU, T. S. (2002) Onset of Asian desertification by 22 Ma ago inferred from loess deposits in China. *Nature,* **416**, 159–163.

HAGER, B. H., R. W. CLAYTON, M. A. RICHARDS, R. P. COMER & A. M. DZIEWONSKI, A.M. (*1985*), *Lower mantle heterogeneity, dynamic topography and the geoid*, *Nature*, ***313***, *541–545*

HALFAR, J. & MUTTI, M. (2005) Global dominance of coralline red-algal facies: A response to Miocene oceanographic events. *Geology,* **33**, 481–484.

HARTLEY, R.A., ROBERTS, G.G., WHITE, N. & RICHARDSON, C. (2011) Transient convective uplift of an ancient burial landscape. *Nature Geoscience,* **4**, 552–565.

HEINE, C., MÜLLER, R.D., STEINBERGER, B. & DICAPIRO, L. (2010) Integrating deep earth dynamics in paleogeographic reconstructions of Australia. *Tectonophysics,* **483**, 135–150.

HERMAN, F., SEWARD, D., VALLA, P.G., CARTER, A., KOHN, B., WILLETT, S.D. & EHLERS, T.A. (2013) Worldwide acceleration of mountain erosion under a cooling climate. *Nature,* **504**, 423–426.

HILGREN , F.J., LOURENS, L.J. & VAN DAM, J.A. (2012) The Neogene Period. In: *The Geologic Time Scale,* (Ed. by F.M. Gradstein, J.G. Ogg, M.D. Schmitz & G.M. Ogg). Elsevier Boston, 932–978.

HOLMES, A. (1929) Radioactivity and earth movements. *Trans. Geol. Soc. Glasgow,* **18**, 559–606.

HOLMES, A. (1944) Principles of physical geology [1st ed.]. Thomas Nelson and Sons, Edinburgh.

HOORN, C., MOSBRUGGER, V., MULCH, A. & ANTONELLI, A. (2013) Biodiversity from mountain building. *Nature Geoscience,* **6**, 154.

HOORN, C., WESSELINGH, F.P., TER STEEGE, H., BERMÚDEZ, M.A., MORA, A., SEVINK, J., SANMARTÍN, I., SANCHEZ-MESEGUER, A., ANDERSON, C.L., FIGUIEREDO, J.P., JARAMILLO, C., RIFF, D., NEGRI, F.R., HOOGHIEMSTRA, H., LUNDBERG, J., STADLER, T., SÄRKINEN, T. & ANTONELLI, A. (2010) Amazonia through time: Andean uplift, climate change, landscape evolution and biodiversity. *Science,* **330**, 927–931.

JONES, S. M., LOVEL, B., & CROSBY, A. G. (2012) Comparison of modern and geological observations of dynamic support from mantle convection. *Journal of the Geological Society of London*, **169,**745-758.

KAIHO, K. (1998) Global climatic forcing of deep sea benthic foraminiferal test size during the past 120 m.y. *Geology,* **26**, 491–494.

KARLSTROM, K.E., COBLENTZ, D., DUEKER, K., OUIMENT, W., … & THE CREST WORKING GROUP (2012) Mantle driven dynamic uplift of the Rocky Mountains and Colorado Plateau and its surface response: Toward a unified hypothesis. *Lithosphere,* **4**, 3–22.

KAUFFMAN, E. G. (1976) Plate tectonics: Major force in evolution. *The Science Teacher*, 43, 12-17.

KELLER, G. & BARRON, J.A. (1983) Paleogeographic implications of Miocene deep-sea hiatuses. *Geol. Soc. Am. Bull.,* **94**, 590–613.

KERR, R.A. (2013) The deep earth machine is coming together. *Science,* **340**, 22–24.

KERRICK, D.M. (2001) Present and past non-anthropogenic CO_2 degassing from the solid earth. *Reviews of Geophysics,* **39**, 565–585.

KESPKA, D.T. (2014) Flights of fancy in avian evolution. *Am. Scientist,* **102**, 34–41.

Kesten, D., Weber, M., Haberland, C., Janssen, C., Agnon, A., Bartov, Y., & DESERT Group. (2008). Combining satellite and seismic images to analyse the shallow structure of the Dead Sea Transform near the DESERT transect. *International Journal of Earth Sciences*, ***97***(**1**), 153-169.

King, P. R. (2000). Tectonic reconstructions of New Zealand: 40 Ma to the present. *New Zealand Journal of Geology and Geophysics*, *43*(4), 611-638.

KOMINZ, M.A. (1984) Oceanic ridge volumes and sea level change—An error analysis. In: *Interregional Unconformities and Hydrocarbon Accumulations,* (Ed. by J.S. Schlee). *Am. Assoc. Pet. Geol. Memoir,* **36**, 109–127.

LEVIN, L.E. (1994) The Oligocene-Neogene sedimentation paradox and plate tectonics. *Trans. Russian Acad. Sci.,* **344**, 158-161. *(Paradoks sedimentatsii v oligotsen-neogene i tektonika plit. Doklady Rossiyskoy Akademii Nauk*, **334**, 739-741.)

LI, GAOJUN, LI, PETTKE, T. & CHEN, J. (2011) Increasing Nd isotopic ratio of Asian dust indicates progressive uplift of the north Tibetan Plateau since the Middle Miocene. *Geology,* **39**, 199-202.

LI, Z-X. & ZHONG, S-J. (2009) Super continent-superplume coupling, true polar wander and plume mobility: Plate dominance in whole mantle tectonics. *Physics of the Earth and Planetary Interiors,* **176**, 143–156, 175.

LIU, L. & STEGMAN, D.R. (2012) Origin of Columbia River flood basalt controlled by propagating rupture of the Farallon slab. *Nature,* **482**, 386–389.

LUEDKE, R.G. & SMITH, R.L. (1984) Map showing distribution, composition, and age of late Cenozoic volcanic centers in western conterminous United States. *U.S. Geol. Surv. Misc. Invest. Ser.,* **I-1833,** 1:2,500,000.

LUSTRINO, M. & WILSON, M. (2007) The circum-Mediterranean anorogenic Cenozoic igneous province. *Earth-Sci. Rev.,* **81**, 1–65.

MARKELLO, J.P., KOEPNICK, R.B., WAITE, L.E. & COLLINS, J.F. (2008) The carbonate analogs through time (CATT) hypothesis and the global atlas of carbonate fields—A systematic and predictive look at Phanerozoic carbonate systems. In: *Controls on Carbonate Platform and Reef Development,* (Ed. by J. Lukasik & J.A. Sima). *SEPM Spec. Paper,* **89**, S15–S45.

Maldonado, A., & Nelson, C. H. (1999). Interaction of tectonic and depositional processes that control the evolution of the Iberian Gulf of Cadiz margin. *Marine Geology*, **155**(1), 217-242.

McNamara, A. K., & Zhong, S. (2005). Thermochemical structures beneath Africa and the Pacific Ocean. *Nature*, ***437***(7062), 1136-1139.

MILLER, K.G., KOMINZ, M.A., BROWNING, J.D., WRIGHT, G.S., MOUNTAIN, M.E., KATZ, P.J., SUGARMAN, B.S., CRAMER, B.S., CHRISTE-BLICK, N. & PEKAR, S.F. (2005) The Phanerozoic record of global sea-level change. *Science,* **310**, 1293–1298.

MISRA, S. & FROELICH, P.N. (2012) Lithium isotope history of Cenozoic seawater: Changes in silicate weathering and reverse weathering. *Science,* **335**, 818–822.

MJELDE, R. & FALEIDE, J.I. (2009) Variation of Icelandic and Hawaiian magmatism: Evidence for co-pulsation of mantle plumes? *Marine Geophysics Resea1rch,* **30**, 61–72.

MOLNAR, P. & ENGLAND, P. (1990) Late Cenozoic uplift of mountain ranges and global climate change: Chicken or egg? *Nature,* **346**, 29–34.

Montes, C., Cardons, A., Jaramillo, C. C., Parde, A., Silva, T.C., Vallensia, V., Ayala, C., Perez-Angel, L. C., Rodriquez-Para, L.A., Ramierz, V.,A. & Nino, H. (2015) Middle Miocene closure of the Central American Seaway, **348,**226- .

Morgan, J.P. & Vannucchi, P. (2014). Earth's fiercely cooling core — 24 TW EGU General Assembly 2014, *Geophysical Research Abstracts*, **16**, EGU2014-14669, 2014.

MOUCHA, R. & FORTE, A.M. (2011) Changes in African topography driven by mantle convection. *Nature Geoscience,* **4**, 707–712.

NORRIS, R.D., TURNER, S.K., HULL, P.M. & RIDGWELL, A. (2013) Marine ecosystem responses to Cenozoic global change. *Science,* **341**, 492–498.

NUNN, J.A. & LIN, G. (2002) Insulating effect of coals and organic rich shales: implications for topography-driven fluid flow, heat transport, and genesis of ore deposits in the Arkoma Basin and Ozark Plateau. *Basin Research*, **14**(2), 129—145.

OWEN, L.A. (2013) Tectonic uplift and continental configurations. In: *The Encyclopedia of Quaternary Science*, (Ed. by S.A. Elias). Elsevier, Amsterdam, **2**, 127–135.

PERRIN, C. (2002) Tertiary: The emergence of modern reef ecosystems. In: *Phanerozoic Reef Patterns*, (Ed. by W. Kiessling, E. Flügel & J. Goloka). *Soc. Sed. Geol. Spec. Pub.,* **72**, 587–621.

PERRIN, C. & KIESSLING, W. (2010) Latitudinal trends in Cenozoic reef patterns and their relationship to climate. *Int. Assoc. Sedimentologists Special Paper,* **42**, 17–34.

PIERCE, K.L. & MORGAN, L.A. (2009) Is the track of the Yellowstone hotspot driven by a deep mantle plume?—Review of volcanism, faulting and uplift in light of new data. *Jour. Volcanology & Geothermal Res.,* **188**, 1–25.

POTTER, P.E. & HAMBLIN, W.K. (2006) Big rivers worldwide: Part 1: Origins: *Brigham Young Univ. Geology Studies,* **48**, 1–36.

POTTER, P.E. & SZATMARI, P. (2009) Global Miocene tectonics and the modern world. *Earth-Sci. Rev.*, **96**, 279–295.

POTTER, P.E. & SZATMARI, P. (2012) Flow diagram relates major earth surface features to the deep earth—Insights from the global Miocene. *Houston Geol. Soc. Bull.*, **55**, 43–55.

Pozzo, M., Davies, C., Gubbins, D., & Alfè, D. (2012). Thermal and electrical conductivity of iron at Earth/'s core conditions. *Nature, **485***(7398), 355-358.

Pozzo, M., Davies, C., Gubbins, D., & Alfè, D. (2014). Thermal and electrical conductivity of solid iron and iron–silicon mixtures at Earth's core conditions. *Earth and Planetary Science Letters, **393***, 159-164.

QUI, J. (2014) Mariners of the lost sea. *Science,* **342**, 130–132.

RAINBIRD, R.H. & ERNST, R.G. (2001) The sedimentary record of mantle plume uplift. In: *Mantle Plumes: Their Identification Through Time*, (Ed. by R.E. Ernst & K.I. Buchan). *Geol. Soc. Amer. Spec. Paper,* **352**, 227–245.

Rögel, Fred (1999) Mediterranean and Paratethys facts and hypotheses of an Oligocene to Miocene paleogeography (short review). Geologica Carpathica, **50**, 339-349.

ROTH, J.M., DROXLER, A.W. & KAMEO, K. (2000) The Caribbean carbonate crash at the middle to late Miocene transitions: Linkage to the establishment of the modern global ocean conveyor (Ed. by R.M. Leckie, H. Sigurdsson, G.D. Acton & G. Draper). *Proc. Ocean Drilling Program Scientific Results,* **165**, 249–273.

RUDDIMAN, W.F., PRELL, W. L., & RAYMO, M. E. (1989) Late Cenozoic uplift in southern Asia and the American west: Rational for general circulation modeling experiments. Jour. Geophysical Research, **94** (18), 379-18391.

SAEMUNDSSON, K. (1986) Subaerial volcanism in the western North Atlantic. In: *The Western North Atlantic region: Decade of North American Geology, v. M* (Ed. By P.R. Vogt, P.R., and B.E.Tucholke), *Geol. Soc. Amer*., 69-86.

SAKAI, T., SANEYOSHI, M., TANAKA, S., SAWADA, Y., NAKATSUKASA, M., MBUA, E. & ISHIDA, H. (2010) Climate shift recorded around 10 Ma in Miocene succession of Samburn Hills, northern Kenya Rift, and its significance. In: *Monsoon: Evolution and Tectonics*, (Ed. by P.D. Clift, R. Tada & H. Zheng). *Geol. Society [London] Spec. Pub.,* **342**, 109–128.

SCHUSTER, M., DURINGER, P., SHIERNA, J.-F., VIGNAUD, P., MACKAYE. H.T., LIKING, A. & BRUNET, M. (2006) The ages of the Sahara desert. *Science,* **311**, 821.

SCLATER, J.G., MEINKE, L., BENNETT, A. & MURPHY, C. (1985) The depth of the ocean through the Neogene. In: *The Miocene Ocean: Paleogeography and Biogeography*, (Ed. by J.F. Kennett). *Geol. Soc. Am. Bull.,* **163**, 1–19.

Scotese, C.R. (2000) Atlas of earth history. Paleomap Project, Arlington, Texas.

SHEPARD, G.E., MÜLLER, R.D., LIU, L. & GURNIS, M. (2010) Miocene drainage reversal of the Amazon River driven by plate-mantle interaction. *Nature Geoscience,* **3**, 870–874.

SMITH, A.G. & PICKERING, K.T. (2003) Oceanic gateways as a critical factor to initiate icehouse Earth. *Jour. Geol. Soc. London,* **160**, 337–340.

SMITH, L.B., JR. & DAVIES, G.R. (2006) Structurally controlled hydrothermal alteration of carbonate reservoirs: Introduction. *AAPG Bull.,* **90**, 1635–1690.

SQUIRES, V.R. (1988) Landscape: A southern hemisphere perspective. *Earth-Sci. Rev.,* **25**, 481–484.

TAKAHASHI, M. & ODA, M. (1997) Geology, tectonics, and integrated stratigraphy potential of Japan. In: *Miocene Stratigraphy: An Integrated Approach*, (Ed. by G.S. Montanari & R. Coccioni). *Developments in Paleontology and Stratigraphy,* **15**, 187–202.

TAMAKI, K. & HONZA, E. (1991) Global tectonics and formation of marginal basins: Role of the western Pacific. *Episodes,* **14**, 224–230.

TCHEREPANOV, E.N., DROXLER, A.W., LAPOINTE, P. & MOHN, K. (2008) Carbonate seismic stratigraphy of the Gulf of Papua mixed depositional system: Neogene stratigraphic signature and eustatic control. *Basin Res.*, **20**, 185–209.

Torsvik, T.H., Smethurst, M.A., Burke, K. & Steinberger, B. (2006) Large igneous provinces generated from the margins of the large low-velocity provinces in the deep mantle. *Geophys. J. Int.* **167** (3), 1447-1460.

VAN UFFORD, Q.A. & CLOOS, M. (2005) Cenozoic tectonics of New Guinea. *AAPG Bull.*, **89**, 119–140.

WAITE, G.P., SMITH, R.P. & ALLEN, R.M. (2006) V_p and V_s structure of the Yellowstone hotspot from teleseismic tomography: Evidence from an upper mantle plume. *Jour. Geophys. Res.*, **111**, 1–21.

WHIPPLE, K.H. (2009) The influence of climate on tectonic evolution of mountain belts. *Nature Geoscience,* **2**, 97–104.

Wichura, H., Bousquet, R., Oberhänsli, R., Strecker, M. R., & Trauth, M. H. (2010). Evidence for middle Miocene uplift of the East African Plateau. *Geology*, ***38***(6), 543-546.

Williams, C. J., Mendell, E. K., Murphy, J., Court, W.M., Johnson, A.H. & Richter, S.I., 2008. Paleoenvironmental reconstruction of a Middle Miocene forest in the western Canadian Arctic. *Paleogeography Paleoclimatology Paleoecology,***262,**160-176.

WILSON, D.S. (1996) Fastest known spreading on the Miocene Cocos-Pacific Plate boundary. *Geophys. Res. Lett.*, **23**, 3003–3006.

WRIGHT, J. D. & MILLER, K.G. (1996) Control of North Atlantic deep water circulation by the Greenland-Scotland Ridge. *Paleoceanography*, **11**, 157-170.

YUAN, H. & DUEKER, K. (2005) Teleseismic P-wave tomogram of the Yellowstone plume, *Geophys. Res. Lemmtt.*, **32**, **4**.

ZACHOS, J., PAGANI, M., SLOAN, L., THOMAS, E. & BILLUPS, K. (2001) Trends, rhythms, and aberrations in global climate 65 Ma to present. *Science,* **292**, 686–693.

ZHANG, N., ZHONG, S., LENG, W. AND LI, Zh-X. (2010). A model for the evolution of the Earth's mantle structure since the Early Paleozoic. *J.Geophys.Res.* **115** B06 401.

ZHANG, Z., RAMSTEIN, G., SCHUSTER, M., LI, CAMILLE, CONTOUX, CAMILLE, AND YAN, Q. (2014). Aridification of the Sahara desert caused by Tethys Sea shrinkage during the Late Miocene. *Nature,* **513,** 401-404.

Ziegler, P. A. (1988). Cenozoic Suturing of Eurasia and Africa-Arabia: Chapter 9, p.121-128. AAPG Memoir 43: Evolution of the Arctic-North Atlantic and the Western Tethys.

Figure Captions

Figure 1. Neogene and Quaternary nomenclature (after Hilgren et al., 2012, p. 946).

Figure 2. Global map of two antipodal superswells over large low shear velocity provinces (LLSVPs); back-arc basins of western Pacific, and late Mesozoic–Tertiary orogenic belts. After Courtillot et al. (2003, Fig. 1), Tamaki and Honza (1991, Fig. 1), and Dickinson et al. (1986, Fig. 1.11). The two superswells may be

thermal plume clusters (superplumes) or thermochemical piles (Bull et al., 2009).

Figure 3. Late Mesozoic – Early Tertiary warm, globe-spanning equatorial current contrasted with today's disjointed and fragmented system (Perrin, 2002, Fig. 5).

Figure 4. Miocene volcanism on the continents: (A) Circum-Mediterranean Cenozoic volcanic regions with histogram of ages. Notice activity in the middle and upper Miocene (Lustrino and Wilson, 2007, Fig. 10, Table 3) and (B) High Lava Plateaus, including the Columbia River basalts in the northwestern United States (Luedke and Smith, 1984) and successively younger, smaller fields ending in Yellowstone Park. These smaller volcanic fields formed as the North American Plate moved over a hotspot (Waite et al., 2006). The Columbia River basalts started at 17 Ma, possibly from a rupture in a descending slab.

Figure 5. Plume under the Yellowstone hotspot (Yuan and Dueker, 2005; Pierce and Morgan, 2009, Fig. 1). Many other hotspots must have had shallow mantle plumes such as this one.

Figure 6. Opening and closing of seven key gateways (Fig. 3) totally disrupted an earlier equatorial global current system and was a key factor in cooling the world ocean, as inferred by δO^{18} isotopes of benthonic forams (Zachos et al., 2001, Fig. 1). Note discontinunity at 15 to 14 Ma.

Figure 7. Idealization of a clinoform in a Tertiary continental embankment (Bartek et al. (1991, Fig.2).

Figure 8. Examples of some Miocene events: (A) Major shift of course of the Amazon River (Hoorn et al., 2010, Fig. 10) and (B) Middle and Upper Miocene deltaic progradation in the North Sea (Cartwright, 1995, Fig. 10).

Figure 9. Progradation of deltas beyond the shelf edges refocuses deposition on slopes prone to failure, especially where they are rich in clay, as in the offshore Pelotas Basin of far southern Brazil (Fontana, 1990, Figs. 2–3). A rapid fall of sea level also promotes overpressure and failure, especially on muddy slopes.

Figure 10. Stable isotope proxies for and late Cretaceous–Cenozoic global tectonics: Left) The stepwise increase in values of isotope δ^7Li measured on benthonic foraminifera (after Misra and Froelich, 2012, Fig. 4b). The sharp rises coincide with orogenic activity and show much more hemipelagic mud transported to the ocean during the middle and late Miocene and Right) a late Cretaceous and Tertiary ^{87}Sr/^{86}Sr curve (Edmond, 1992, Fig. 1).

Figure 11. Uplift of East Africa starting in the middle to late Miocene established the conditions for early hominids (Sakai et al., 2010, Fig. 9).

Figure 12. Model of mantle dynamics across the Pacific, based on S-wave seismic velocities and petrologic studies. Catastrophic collapse of stagnant subducted oceanic lithosphere (green) in eastern Asia at 20-30 Ma formed a high-velocity D" layer (blue) at the core-mantle boundary (CMB). Heating by the core removed this D" layer in the southern Pacific, transforming it into a superplume of rising andesitic solids (brown) in the lower mantle

and above it the Pacific superswell; dense residual melts sank to the CMB forming an ultra-low velocity zone – ULVZ. Pv – perovskite; pPv – post-perovskite. (After Maruyama et al., 2007, Fig. 6).

Figure 13. Modern hotspots tend to occur along the borders of the African and Pacific Large Low Shear Velocity Provinces of the lowermost mantle (Li and Zhong, 2009, Fig. 11).

Figure 14. Schematic diagram of evolution of a cratonic, marine basin above a shallow mantle plume (after Rainbird and Ernst, 2001, Fig. 8).

Figure 15. Flow diagram connects deep earth cycle to major features of earth surface paleogeography. Although many important feedback loops are not shown, understanding the underlying causal dependence of major surface processes to tectonics is critical to seeing how the earth machine works (modified from Potter and Szatmari, 2009).

Figure 1

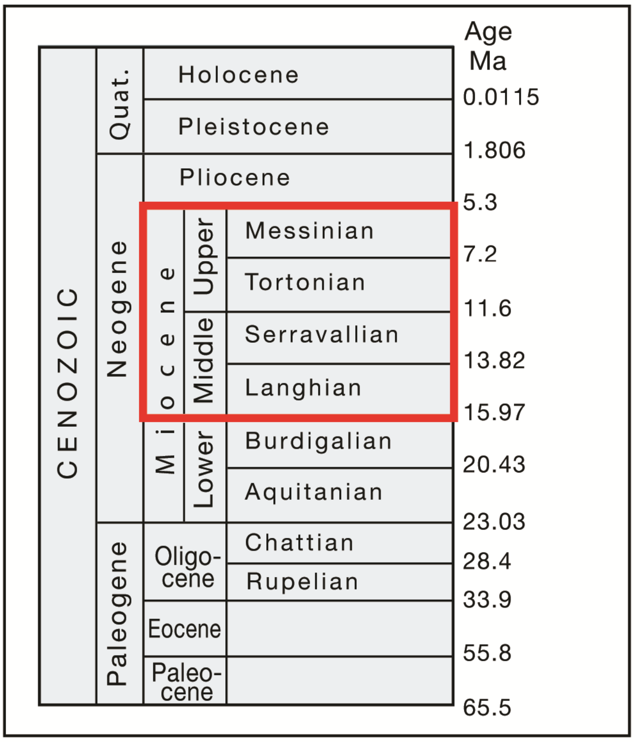
Age
Ma
CENOZOIC
Quat.
Neogene
Paleogene
Miocene
Upper
Middle
Lower
Holocene
Pleistocene
Pliocene
Messinian
Tortonian
Serravallian
Langhian
Burdigalian
Aquitanian
Oligo-
cene
Chattian
Rupelian
Eocene
Paleo-
cene
0.0115
1.806
5.3
7.2
11.6
13.82
15.97
20.43
23.03
28.4
33.9
55.8
65.5

B. R.
Figure 2

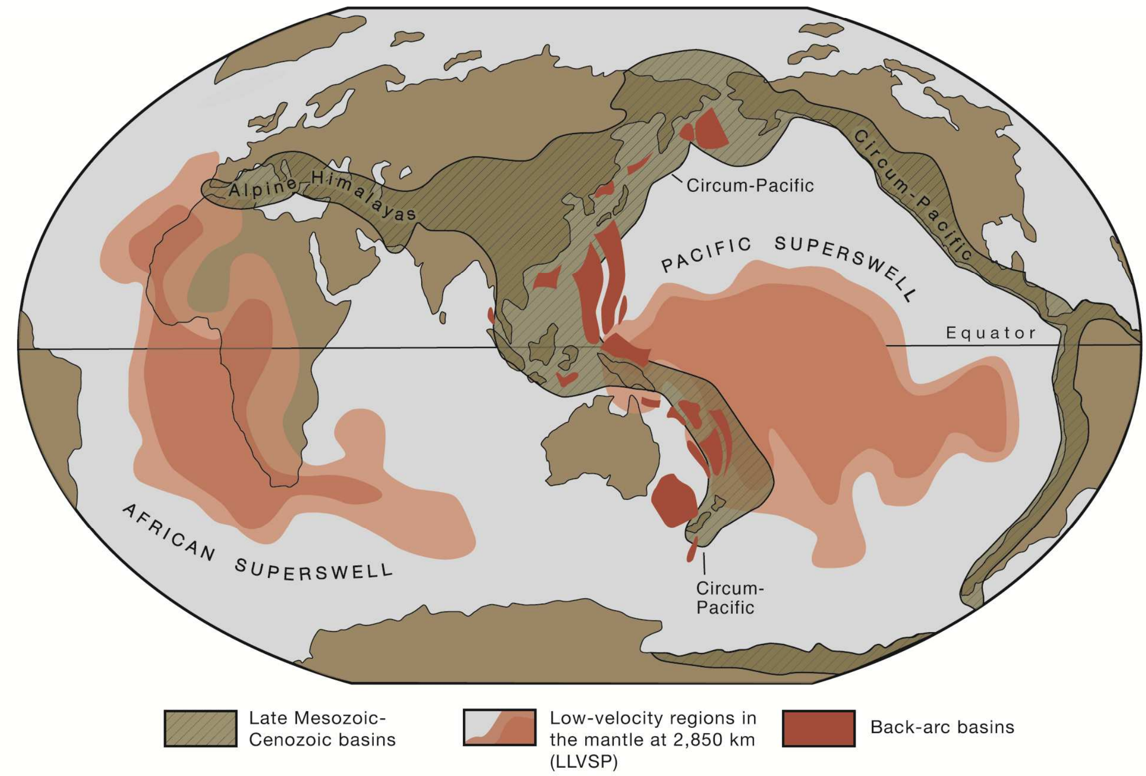
Alpine-Himalayas
Circum-Pacific
Circum-Pacific
PACIFIC SUPERSWELL
Equator
AFRICAN SUPERSWELL
Circum-Pacific
Late Mesozoic-Cenozoic basins
Low-velocity regions in the mantle at 2,850 km (LLVSP)
Back-arc basins

B. R.
Figure 3

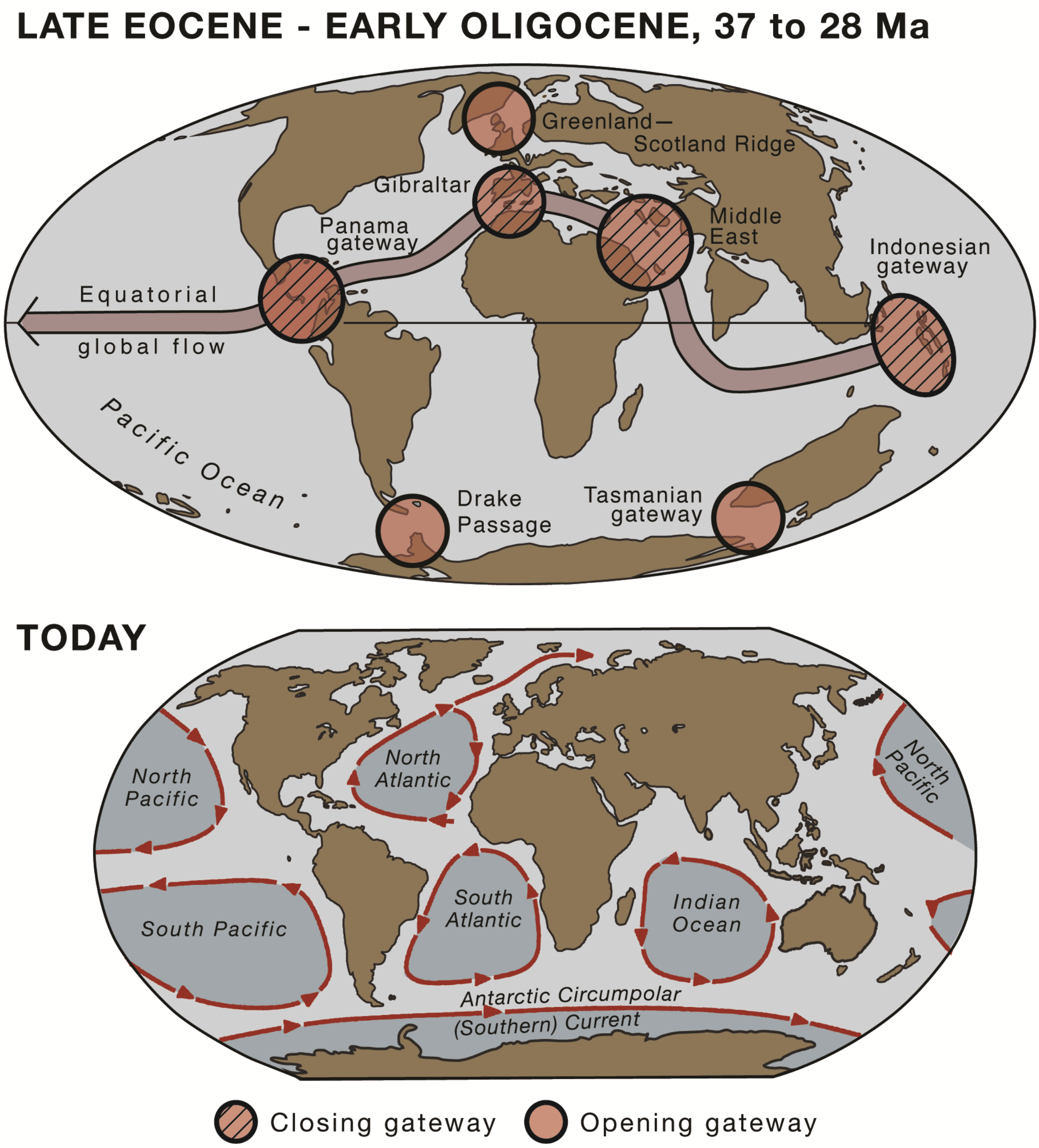

LATE EOCENE - EARLY OLIGOCENE, 37 to 28 Ma
Greenland—
Scotland Ridge
Gibraltar
Panama
gateway
Middle
East
Indonesian
gateway
Equatorial
global flow
Pacific Ocean
Drake
Passage
Tasmanian
gateway
TODAY
North
Pacific
North
Atlantic
North
Pacific
South
Atlantic
Indian
Ocean
South Pacific
Antarctic Circumpolar
(Southern) Current
Closing gateway
Opening gateway

B. R.
Figure 4

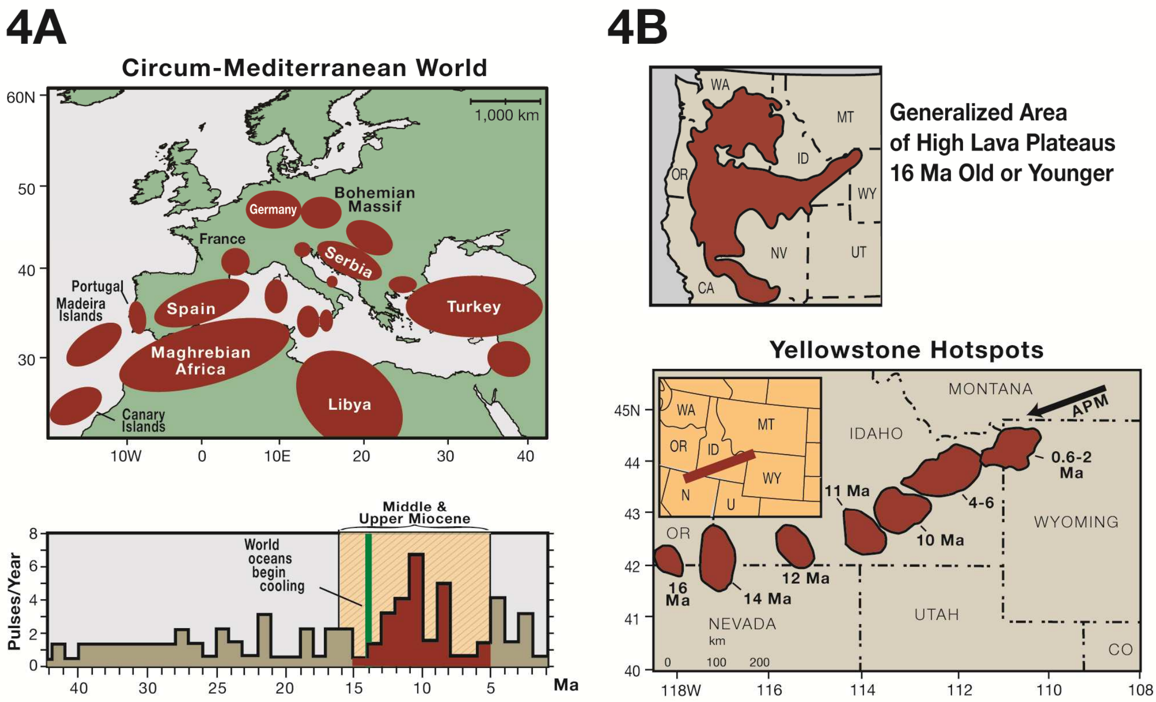
4A
Circum-Mediterranean World
60N
50
40
30
1,000 km
Germany
Bohemian Massif
France
Serbia
Portugal
Madeira Islands
Spain
Turkey
Maghrebian Africa
Libya
Canary Islands
10W
0
10E
20
30
40
Middle & Upper Miocene
World oceans begin cooling
Pulses/Year
8
6
4
2
0
40
30
25
20
15
10
5
Ma
4B
WA
MT
ID
OR
WY
NV
UT
CA
Generalized Area of High Lava Plateaus 16 Ma Old or Younger
Yellowstone Hotspots
MONTANA
APM
IDAHO
WA
MT
OR
ID
WY
N
U
45N
44
43
42
41
40
0.6-2 Ma
11 Ma
4-6
10 Ma
WYOMING
OR
16 Ma
14 Ma
12 Ma
NEVADA
UTAH
CO
km
0
100
200
118W
116
114
112
110
108

B.R.
Figure 5

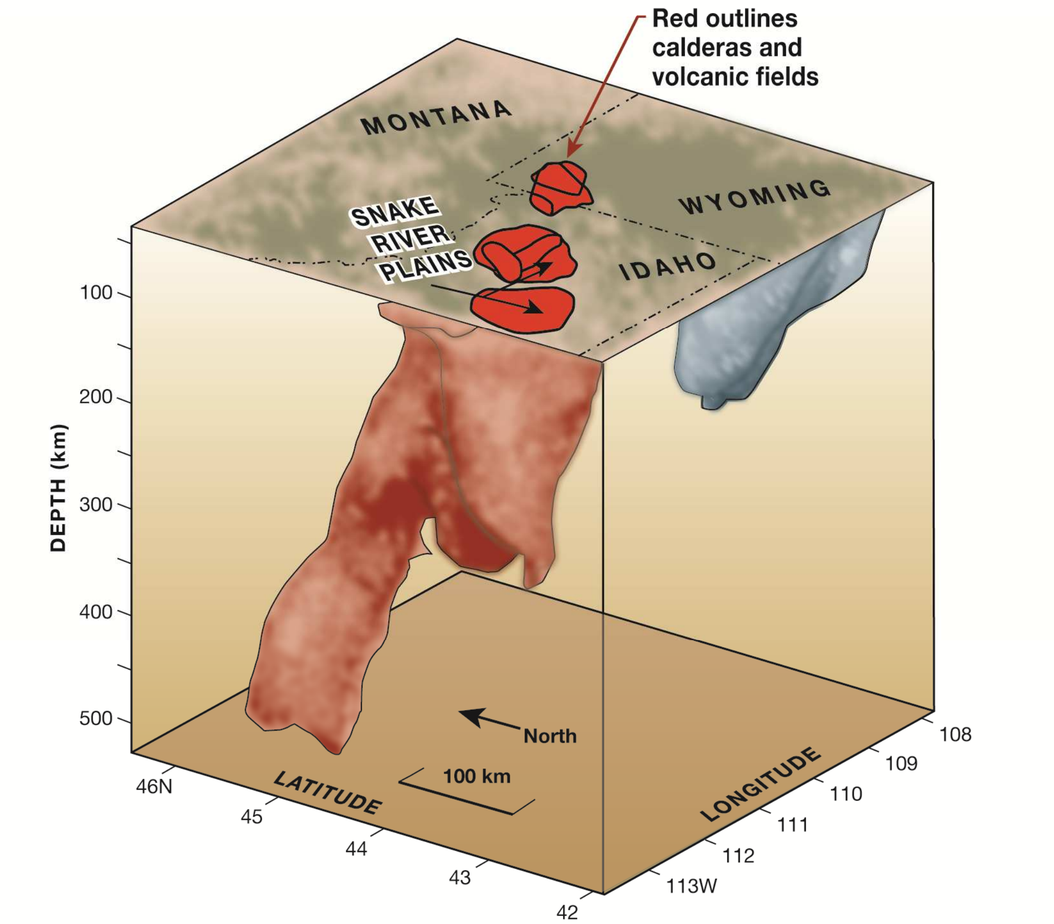
Red outlines calderas and volcanic fields
MONTANA
WYOMING
IDAHO
SNAKE RIVER PLAINS
DEPTH (km)
100
200
300
400
500
North
100 km
LATITUDE
46N
45
44
43
42
LONGITUDE
108
109
110
111
112
113W

B.R.
Figure 6

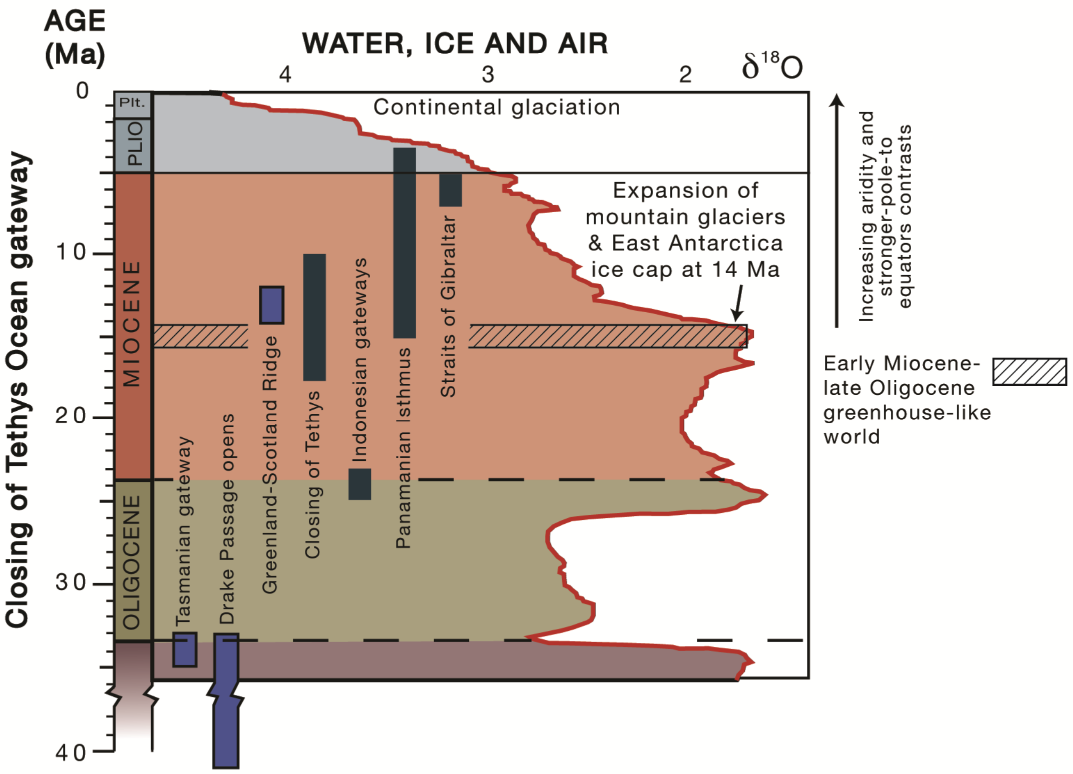
AGE
(Ma)
WATER, ICE AND AIR
δ18O
4
3
2
0
10
20
30
40
Plt.
PLIO
MIOCENE
OLIGOCENE
Continental glaciation
Expansion of mountain glaciers & East Antarctica ice cap at 14 Ma
Closing of Tethys Ocean gateway
Tasmanian gateway
Drake Passage opens
Greenland-Scotland Ridge
Closing of Tethys
Indonesian gateways
Panamanian Isthmus
Straits of Gibraltar
Increasing aridity and stronger-pole-to equators contrasts
Early Miocene-late Oligocene greenhouse-like world

B.R.
Figure 7

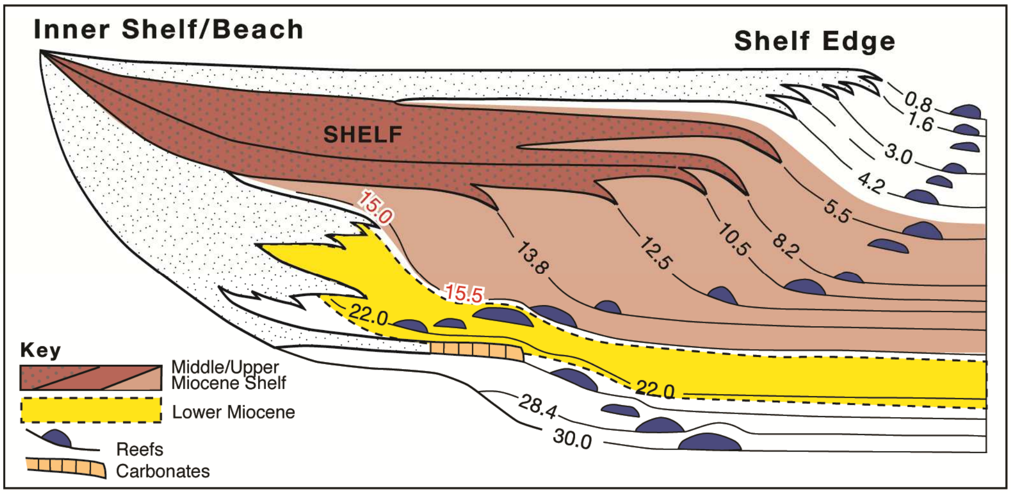
Inner Shelf/Beach
Shelf Edge
SHELF
0.8
1.6
3.0
4.2
5.5
8.2
10.5
12.5
13.8
15.0
15.5
22.0
22.0
28.4
30.0
Key
Middle/Upper Miocene Shelf
Lower Miocene
Reefs
Carbonates

B.R.
Figure 8 A & B

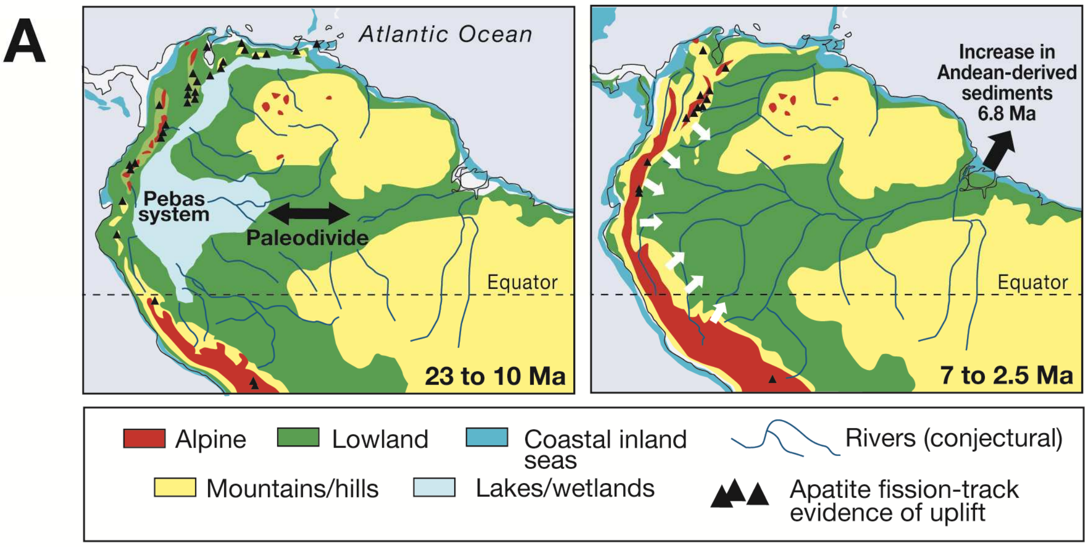

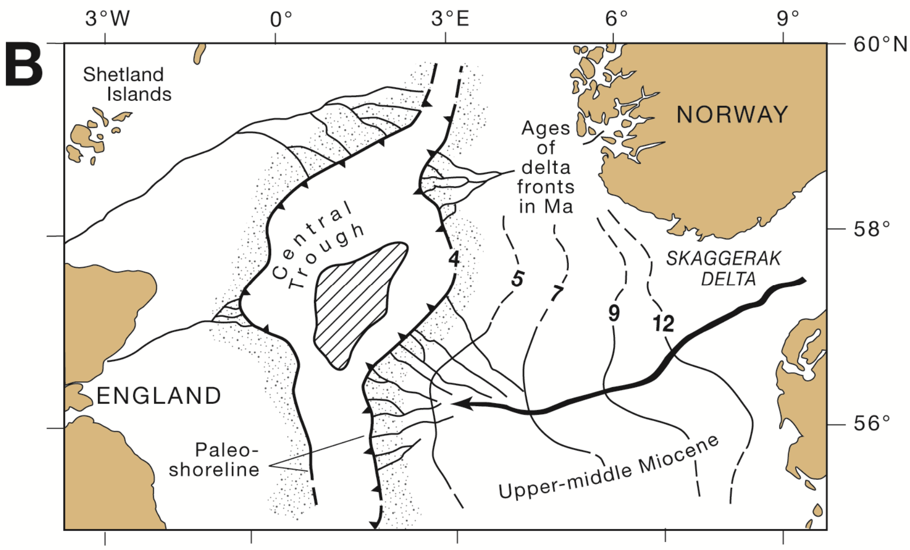

B. R.
Figure 9 A & B

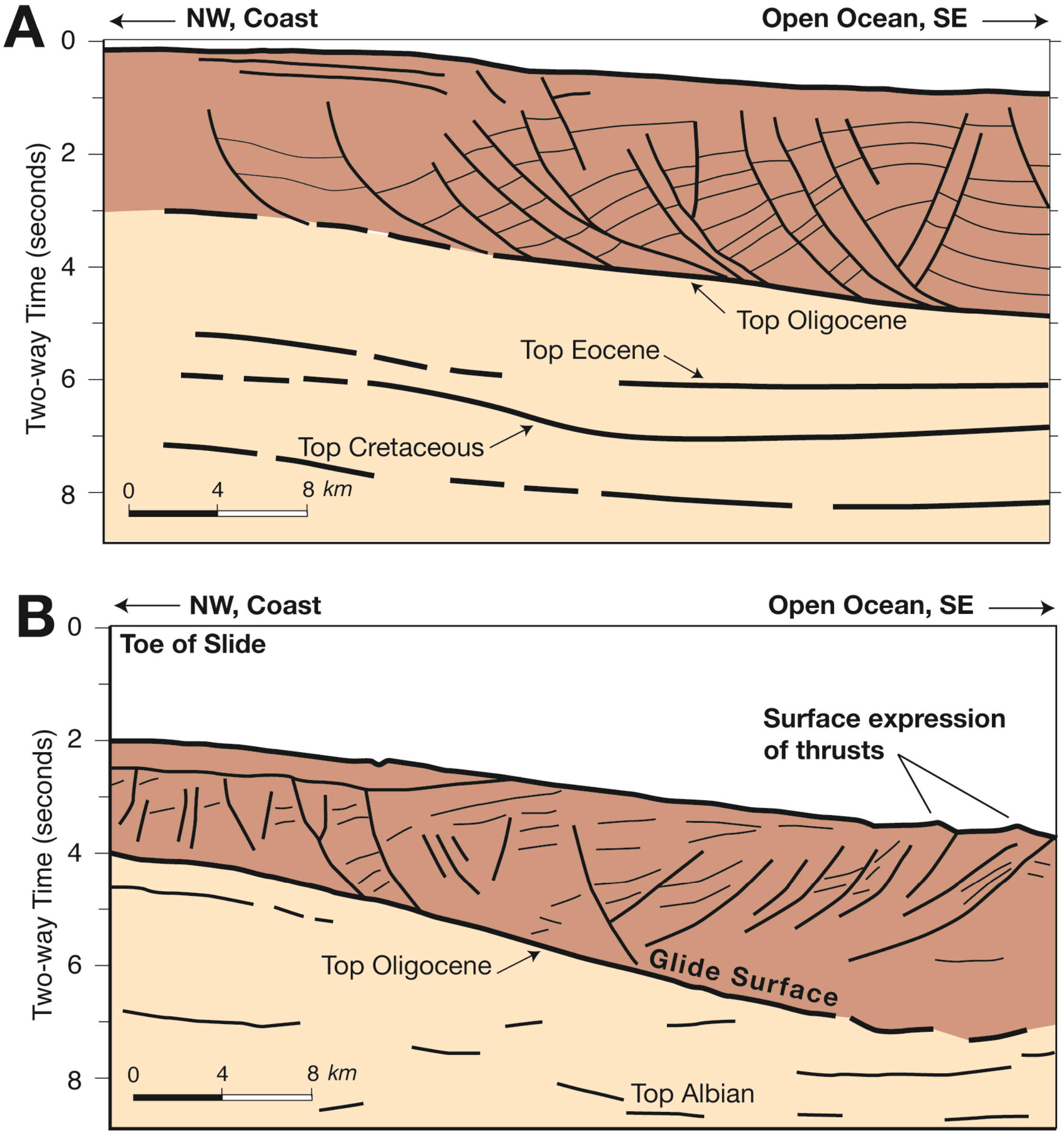

B. R.
Figure 10

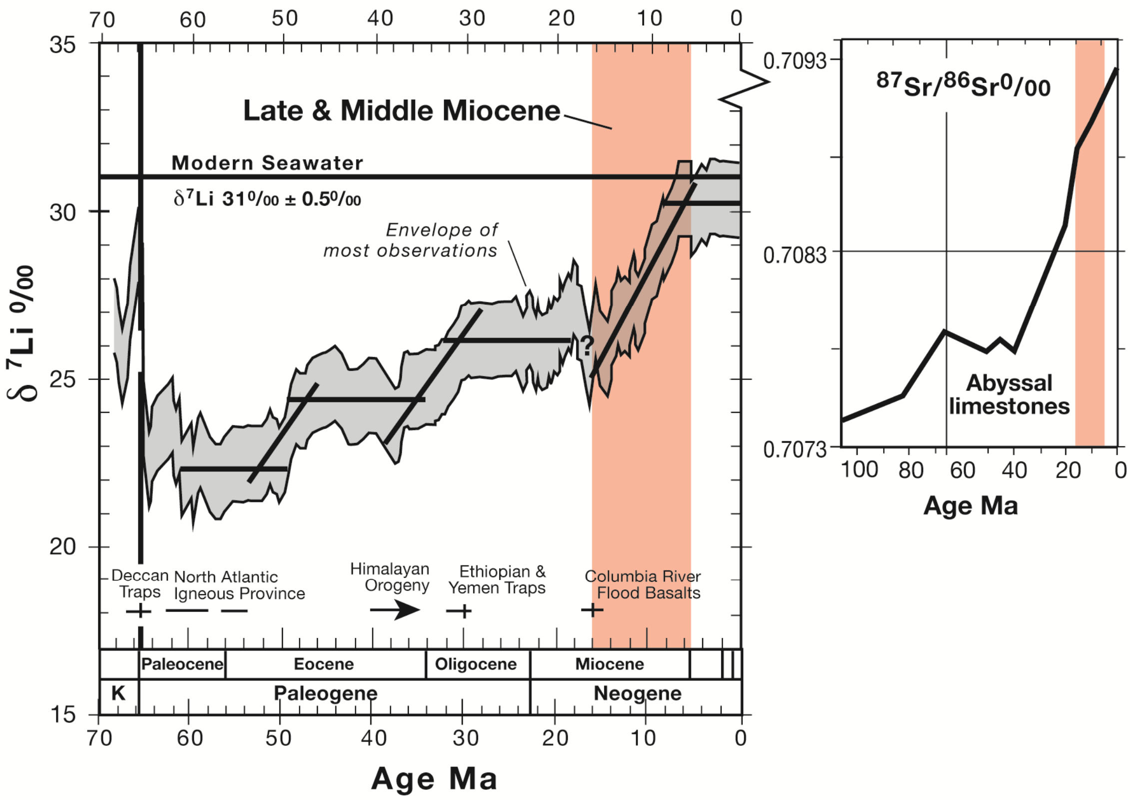
Late & Middle Miocene
Modern Seawater
δ7Li 31‰ ± 0.5‰
Envelope of most observations
δ 7Li ‰
Deccan Traps
North Atlantic Igneous Province
Himalayan Orogeny
Ethiopian & Yemen Traps
Columbia River Flood Basalts
Paleocene
Eocene
Oligocene
Miocene
K
Paleogene
Neogene
Age Ma
87Sr/86Sr‰
Abyssal limestones
Age Ma

B. R.
Figure 11

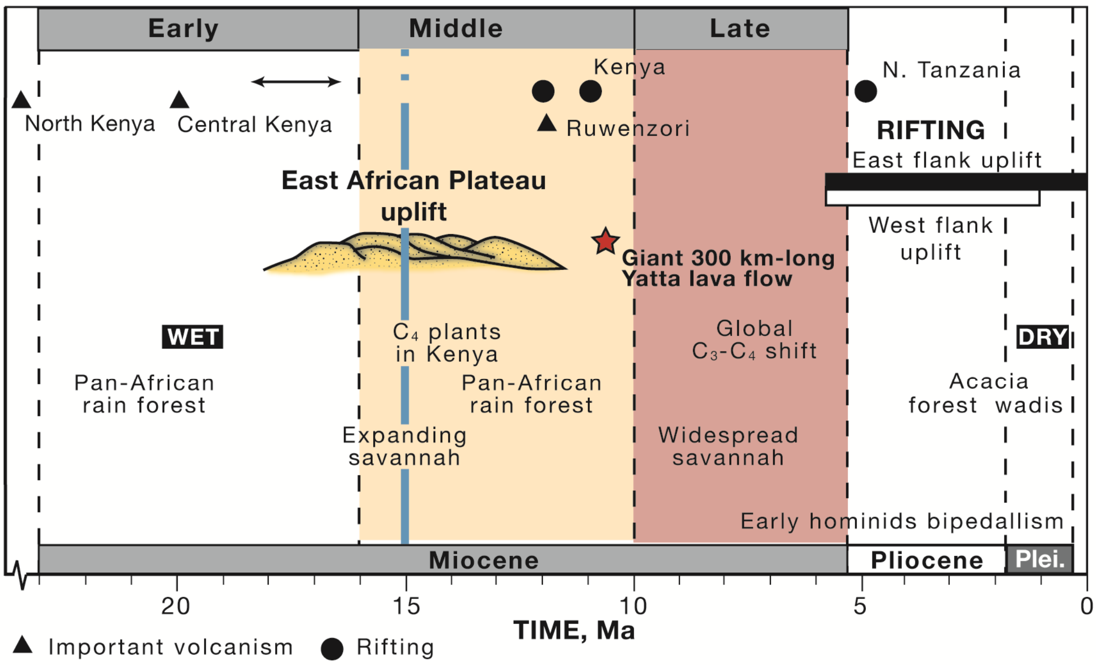
Early
Middle
Late
North Kenya
Central Kenya
Kenya
Ruwenzori
N. Tanzania
RIFTING
East flank uplift
West flank uplift
East African Plateau uplift
Giant 300 km-long Yatta lava flow
WET
Pan-African rain forest
C4 plants in Kenya
Pan-African rain forest
Expanding savannah
Global C3-C4 shift
Widespread savannah
DRY
Acacia forest wadis
Early hominids bipedallism
Miocene
Pliocene
Plei.
20
15
10
5
0
TIME, Ma
Important volcanism
Rifting

Figure 12

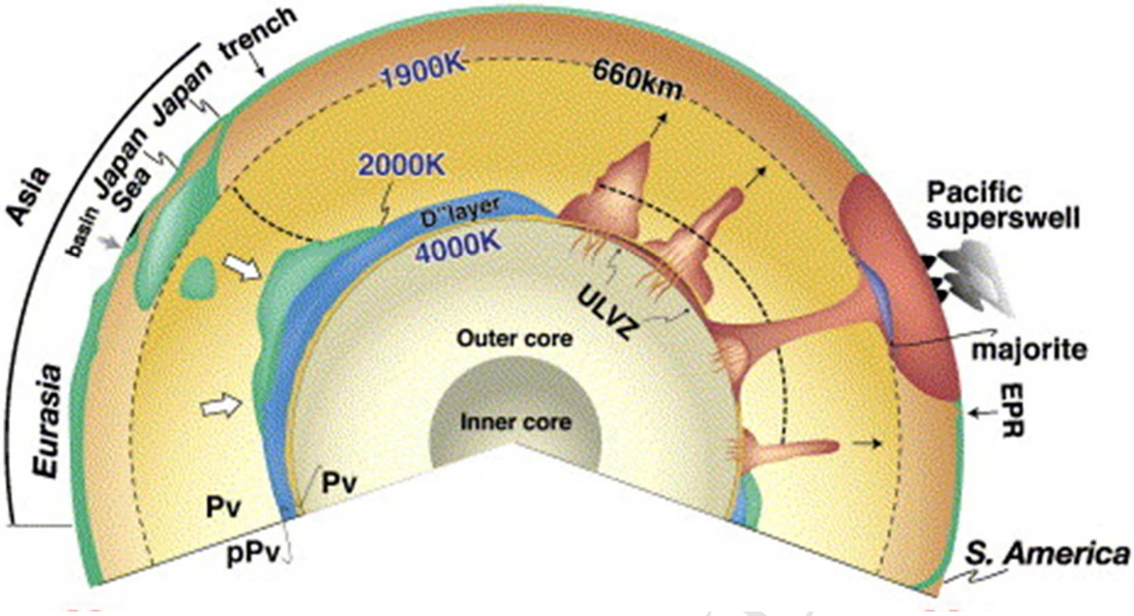
trench
Japan
Japan
Sea
basin
Asia
Eurasia
1900K
660km
2000K
D''layer
4000K
Outer core
Inner core
ULVZ
Pv
Pv
pPv
Pacific
superswell
majorite
EPR
S. America

B. R.
Figure 13

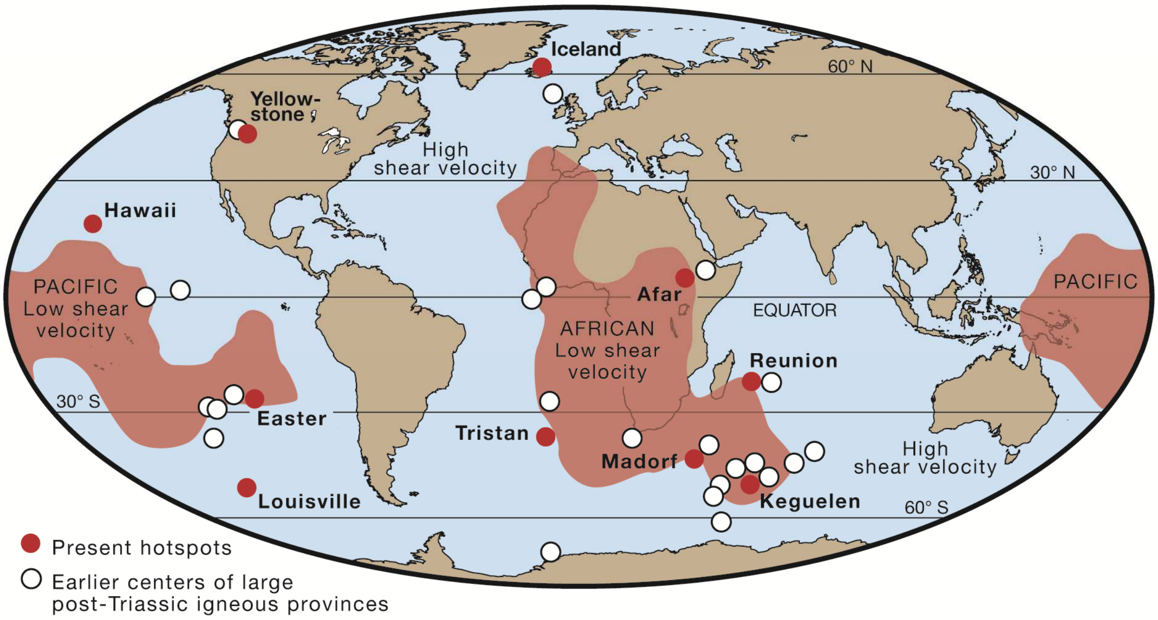

Iceland
60° N
Yellow-
stone
High
shear velocity
30° N
Hawaii
PACIFIC
Low shear
velocity
Afar
EQUATOR
PACIFIC
AFRICAN
Low shear
velocity
Reunion
30° S
Easter
Tristan
Madorf
High
shear velocity
Louisville
Keguelen
60° S
Present hotspots
Earlier centers of large
post-Triassic igneous provinces

B. R.
Figure 14

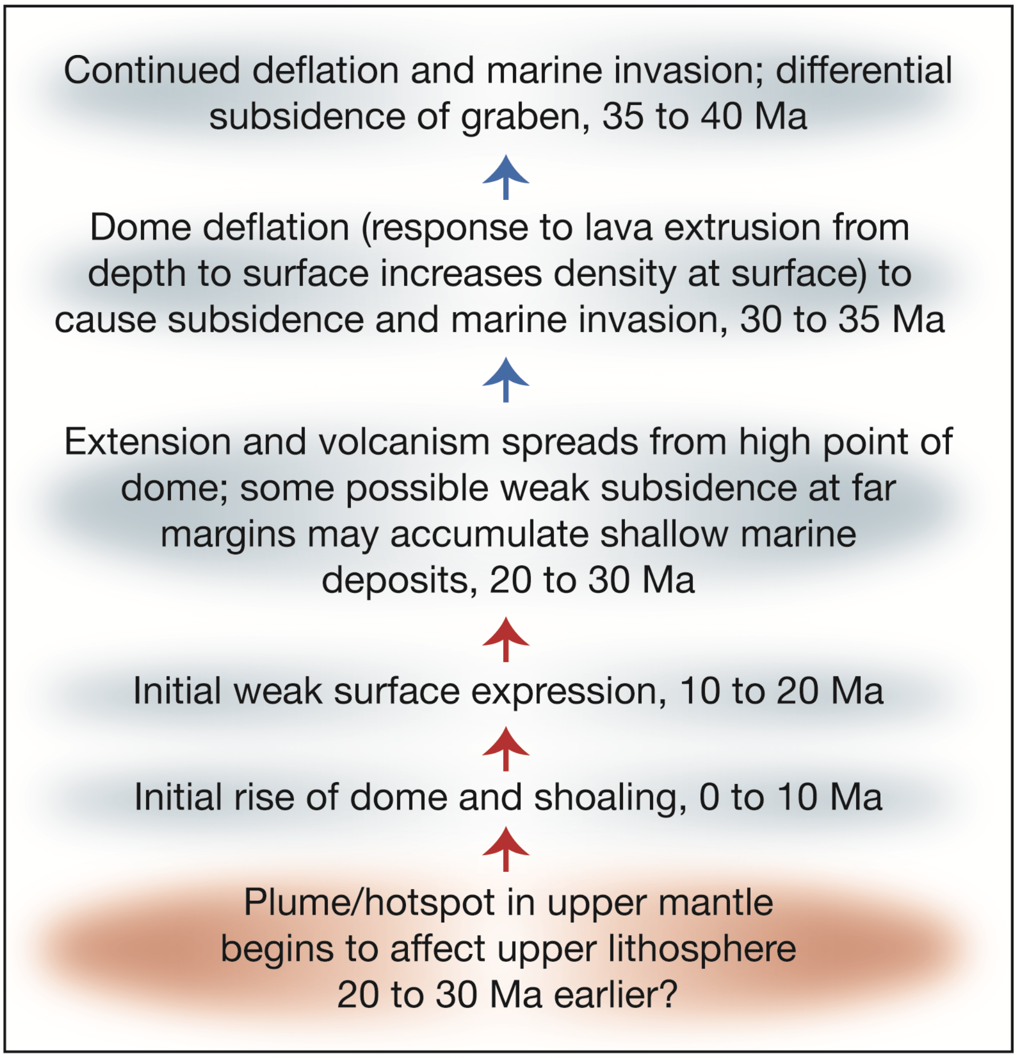
Continued deflation and marine invasion; differential subsidence of graben, 35 to 40 Ma
Dome deflation (response to lava extrusion from depth to surface increases density at surface) to cause subsidence and marine invasion, 30 to 35 Ma
Extension and volcanism spreads from high point of dome; some possible weak subsidence at far margins may accumulate shallow marine deposits, 20 to 30 Ma
Initial weak surface expression, 10 to 20 Ma
Initial rise of dome and shoaling, 0 to 10 Ma
Plume/hotspot in upper mantle begins to affect upper lithosphere 20 to 30 Ma earlier?

Figure 15

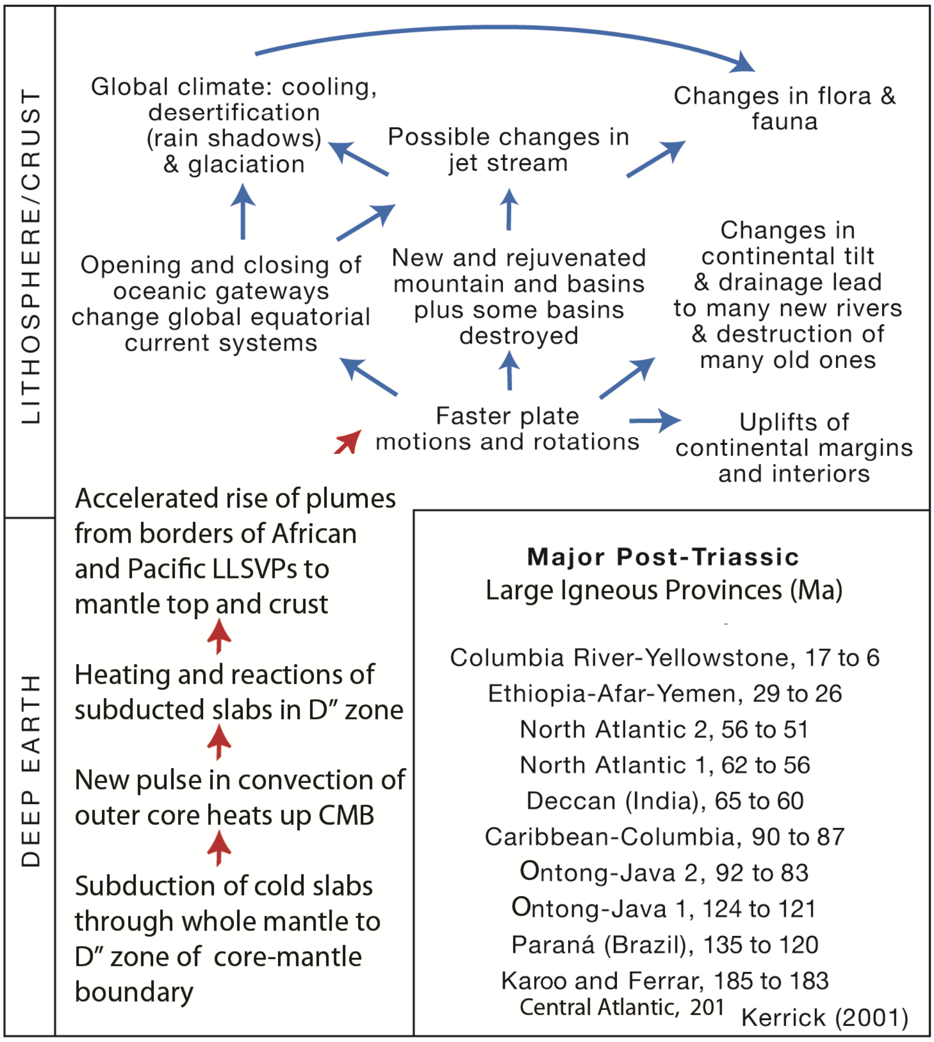
LITHOSPHERE/CRUST
DEEP EARTH
Global climate: cooling, desertification (rain shadows) & glaciation
Possible changes in jet stream
Changes in flora & fauna
Opening and closing of oceanic gateways change global equatorial current systems
New and rejuvenated mountain and basins plus some basins destroyed
Changes in continental tilt & drainage lead to many new rivers & destruction of many old ones
Faster plate motions and rotations
Uplifts of continental margins and interiors
Accelerated rise of plumes from borders of African and Pacific LLSVPs to mantle top and crust
Heating and reactions of subducted slabs in D" zone
New pulse in convection of outer core heats up CMB
Subduction of cold slabs through whole mantle to D" zone of core-mantle boundary
Major Post-Triassic
Large Igneous Provinces (Ma)
Columbia River-Yellowstone, 17 to 6
Ethiopia-Afar-Yemen, 29 to 26
North Atlantic 2, 56 to 51
North Atlantic 1, 62 to 56
Deccan (India), 65 to 60
Caribbean-Columbia, 90 to 87
Ontong-Java 2, 92 to 83
Ontong-Java 1, 124 to 121
Paraná (Brazil), 135 to 120
Karoo and Ferrar, 185 to 183
Central Atlantic, 201
Kerrick (2001)

Highlights

Near-global orogenies occurred in Eurasia and the Circumpacific in only 11 Ma.

Major events affected global tectonics, volcanism, lands, oceans, climate, biology.

More active plate tectonics raised mountains, opened and closed key oceanic gateways.

These events transformed a lingering greenhouse world into an icehouse world.

The ultimate cause was a pulse of heat from Earth's core transmitted by mantle plumes.